6
Pulmonary Effects of Carbon Nanomaterials

Liying Wang, Donna C. Davidson, Vincent Castranova, and Yon Rojanasakul

6.1
Introduction

Carbon nanomaterials, a class of small-scale (<100 nm) carbon-based materials formed by molecular-level engineering with unique mechanical, optical, and electrical properties, have increasingly been utilized for a wide range of applications in such as electronics, energy storage, structural materials, pharmaceuticals, cosmetics, agriculture, medical diagnostics, and drug delivery [1–3]. The chemistry of pure carbon particles is surprisingly uninteresting, since they are significantly unreactive. However, there are some types of carbon nanomaterials, such as carbon nanotubes (CNTs), which are more reactive than others because of the defects from missing carbon atoms and the more strained curved-end caps [4]. Additionally, nano-scale materials have a high surface area-to-volume ratio in comparison to their bulk counterparts, which leads to their high reactivity as well as biological activities following intended and unintended exposure to sensitive mammalian tissue.

Because of the small size and low density of carbon nanoparticles (NPs), aerosolization is likely during energetic processes such as vortexing, weighing, sonication, mixing, and blending [5–8]. Thus, human exposure via inhalation is anticipated during the production, usage, and disposal of nanoparticles [9]. As a result, the lung is the major target organ for aerosolized nanoparticle exposure. Consistently, the respiratory system represents a unique target for the potential toxicity of nanoparticles due to the fact that, in addition to being the portal of entry for inhaled particles, it also receives the entire cardiac output. As such, there is potential for exposure of the lungs to nanoparticles resulting in particle translocation to extrapulmonary organs via systemic circulation. Nanomaterials may also enter the lung via other exposure routes including dermal and gastrointestinal absorption or direct injection.

In response to inhaled airborne particles, biological defense of the lung occurs [10]. In general, alveolar macrophages and epithelial cells are the two major

Biomedical Applications and Toxicology of Carbon Nanomaterials, First Edition.
Edited by Chunying Chen and Haifang Wang.
© 2016 Wiley-VCH Verlag GmbH & Co. KGaA. Published 2016 by Wiley-VCH Verlag GmbH & Co. KGaA.

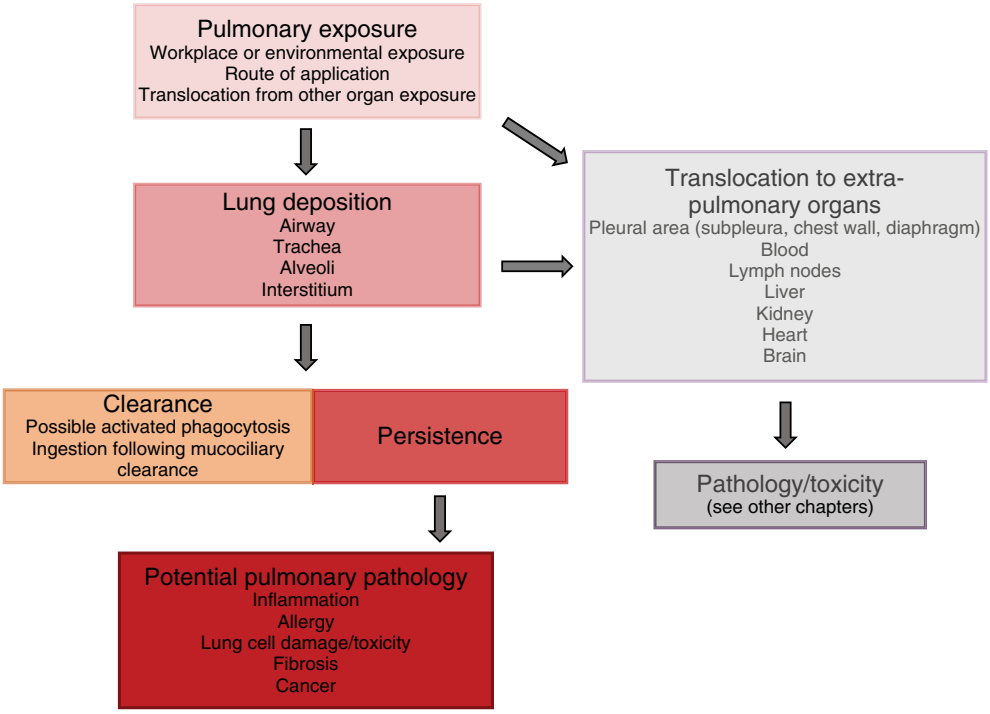

Figure 6.1 Overall fate and toxicity potential of pulmonary-exposed CNTs.

resident cells that interact with inhaled particles in the alveolar region of the lung. Classically, pulmonary responses to inhaled insoluble particles include physiological defense mechanisms, such as clearance, as well as pathological response mechanisms, such as inflammation, oxidative stress, cell damage, aberrant proliferation, and lung tissue remodeling, which may lead to the development of lung fibrosis. However, studies have found that nanomaterials deposited in the lungs, including carbon nanoparticles, show a different behavior compared to fine particles of the same chemical composition (Figure 6.1). In this chapter, the unique bioactivities of nanomaterials exposed to the lungs will be discussed.

6.2 Physicochemical Properties of Carbon Nanomaterials

Nanoparticles exhibit unique physicochemical properties and are likely to exhibit biological activities that are significantly different from those by fine or micrometer-sized particles of the same chemical composition. These properties, such as the particle size, shape, solubility, charge, and surface reactivity, are

10.1002/9783527692866.ch6, Downloaded from https://onlinelibrary.wiley.com/doi/10.1002/9783527692866.ch6 by NASA Shared Services Center (NSSC), Wiley Online Library on [19/05/2023]. See the Terms and Conditions (https://onlinelibrary.wiley.com/terms-and-conditions) on Wiley Online Library for rules of use; OA articles are governed by the applicable Creative Commons License

believed to be important determinants of the biological responses [11, 12]. For example, a large body of literature suggests that the fiber-like CNTs may have unusual toxicity properties. In particular, CNTs seem to have a special ability to stimulate mesenchymal cell growth and cause granuloma formation and fibrogenesis, causing more adverse effects than the same mass of NP carbon and quartz, the latter a commonly used benchmark of particle toxicity [13]. In addition to the particle characteristics mentioned above, the bioactivities of NPs also depend on particle oxidant generation, surface functionalization, and the rate of dissolution. Changes in physicochemical reactivity of NPs also cause them to interact with circulatory and cellular proteins differentially, leading to their altered biokinetic profiles, including adsorption, distribution, translocation, transformation, and elimination [14].

When assessing the respiratory toxicity of nanomaterials through inhalation, intratracheal instillation, or pharyngeal aspiration, discrepancies observed among these administration routes can result from differences in the physiochemical properties of the nanomaterials themselves, such as agglomeration and dispersion. Therefore, it is essential that identification and characterization of the NPs' physicochemical properties be performed in all toxicity studies [15]. Examples of these physicochemical parameters and how they affect the bioactivities of carbon nanomaterials are discussed below.

6.2.1
Types of Carbon Nanomaterials

Commonly studied classes of carbon nanoparticles include fullerenes, graphene, CNTs, carbon nanofibers (CNFs), and ultrafine carbon black (UFCB). Fullerenes are hollow balls of carbon, while graphene consists of carbon that is arranged in flat sheets. In the case of CNTs, carbon is arranged in a cylindrical structure. CNTs are further subdivided based on the number of carbon layers that make up the nanotubes; that is, one ("single-walled carbon nanotube"; SWCNT), two ("double-walled carbon nanotube"; DWCNT), or several ("multi-walled carbon nanotube"; MWCNT) layers. CNTs range from one to several nanometers in width and up to several micrometers in length. This large length-to-width (aspect) ratio, a property shared with asbestos fibers, has led to concerns that inhaled CNTs may cause asbestos-like pathologies, such as pulmonary fibrosis and lung cancer [16]. CNFs differ from CNTs in that they are usually larger in diameter and noncontinuous, containing exposed graphene edge planes [17]. UFCB represents the nano-sized portion of carbon black (CB) materials, and is often used as surrogate for nano-scaled particulate matter found in ambient air.

6.2.2
Effects of Size

When the dimension of a solid material becomes very small, its physical and chemical properties can be very different from those of the same material in its

10.1002/9783527692866.ch6 Downloaded from https://onlinelibrary.wiley.com/doi/10.1002/9783527692866.ch6 by NASA Shared Services Center (NSSC), Wiley Online Library on [19/05/2023]. See the Terms and Conditions (https://onlinelibrary.wiley.com/terms-and-conditions) on Wiley Online Library for rules of use; OA articles are governed by the applicable Creative Commons License

bulk form. A growing body of data indicates that particle size is an important factor in determining the biological response to particles. Accordingly, the bioactivity of MWCNTs has been shown to increase with both their diameter and length [18]. Xu *et al.* utilized an exposure period of 24 weeks to determine whether the size and shape of MWCNTs impact deposition and lesion development in the lung pleura [14]. Using two different types of MWCNT, namely a large, needle-like MWCNT (length = 8 μm, diameter = 150 nm) and a small MWCNT (length = 3 μm, diameter = 15 nm), administered to the lungs of rats once every 2 weeks for 24 weeks by transtracheal intrapulmonary spraying, the authors noted that the large MWCNTs – but not the small ones – translocated into the pleural cavity, deposited in the parietal pleura, and induced fibrosis with occasional parietal mesothelial proliferative lesions. In addition, the large MWCNTs induced a greater number of inflammatory cells in the pleural lavage, while the small MWCNTs induced stronger inflammation and higher 8-hydroxydeoxyguanosine level in the lung tissue. Collectively, these results suggest that the large MWCNTs may pose a greater risk of pleural lesions relevant to mesothelioma development, similar to asbestos [14].

In addition to affecting the distribution in tissue, the size of particles can influence their toxicity. In general, small particles exert harmful effects as a consequence of two factors that act together to contribute to their toxicity: surface area and the intrinsic reactivity or toxicity of that surface [19, 20]. The smaller the particles, the more their surface area per unit mass and, consequently, the more the enhancement in the intrinsic toxicity of the particle surface [21]. Therefore, as the particles become smaller, their likelihood of causing harm to the lung tissue increases.

Interestingly, Poulsen *et al.* [22] found that exposure of mice to small or large MWCNTs resulted in a similar global transcription pattern, with both MWCNTs eliciting strong acute-phase and inflammatory responses that peaked at day 3 and persisted up to 28 days and were characterized by a large number of inflammatory cells in the bronchoalveolar lavage fluid, interstitial pneumonia, and gene expression changes. However, exposure to large CNTs resulted in a faster onset of inflammation and DNA damage, and caused more fibrosis with a unique fibrotic gene signature at day 28, as compared to small CNTs [22].

6.2.3
Effects of Agglomeration State

Nanoparticles are often dispersed in aqueous media, the composition of which may differ substantially depending on their applications, in order to deliver the particles to the *in vitro* or *in vivo* systems of interest. However, nanoparticles may or may not disperse well in these media, and likewise may not disperse to the same extent in the same medium, depending on their physicochemical properties. Therefore, the particles may be delivered as agglomerates of various structures and sizes of the nanomaterial. Accordingly, the agglomeration state has been demonstrated to impact the bioactivities of nanomaterials as elaborated below.

10.1002/9783527692866.ch6, Downloaded from https://onlinelibrary.wiley.com/doi/10.1002/9783527692866.ch6 by NASA Shared Services Center (NSSC), Wiley Online Library on [19/05/2022]. See the Terms and Conditions (https://onlinelibrary.wiley.com/terms-and-conditions) on Wiley Online Library for rules of use; OA articles are governed by the applicable Creative Commons License

Several studies have shown that exposure to well-dispersed CNTs can have different pathological outcomes as compared to agglomerated CNTs. For example, pulmonary aspiration of large agglomerates of SWCNTs (~15 μm in diameter) resulted in structures that remained in the alveolar airspaces and ultimately induced inflammatory granulomas with SWCNT agglomerates, encased by epithelioid macrophages. In contrast, well-dispersed SWCNTs (D-SWCNTs, mean diameter of 0.69 μm) did not produce granulomas encased by epithelioid macrophages; rather, they induced a more potent interstitial fibrotic response. The latter was also observed to be associated with minimal lung inflammation and macrophage engulfment of D-SWCNTs [23–25]. This suggests that the ability of small D-SWCNT structures to escape macrophage phagocytosis and enter the lung interstitium could be a key determining factor in the relative absence of macrophage-derived lung inflammation and oxidant stress and the enhanced induction of interstitial fibrosis by D-SWCNTs. Because lung fibrosis caused by D-SWCNTs occurs quite rapidly in the absence of sustained inflammatory and oxidative stress responses, traditional *in vitro* screening tests, which are based on cytotoxicity and oxidative stress detection, are generally inadequate for predicting the *in vivo* fibrogenicity of SWCNTs [23–25].

The study described above also revealed that large micrometer-sized agglomerates deposited mainly in the proximal alveolar region, while the small D-SWCNT structures deposited largely in the distal alveoli and rapidly entered the alveolar walls [23]. These data further emphasize the extent to which the bioactivity of a nanomaterial can be affected by the degree to which the nanoparticles are agglomerated, that is, the physical size of the nanoparticle structures as they interact with biological systems. A similar finding was observed with UFCB by Shvedova *et al*. (2007)[26], who reported that intratracheal instillation of well-dispersed CB nanoparticles resulted in an eightfold increase in pulmonary response as compared to agglomerated CB nanoparticles of equal mass burden. Collectively, these studies highlight the pressing need to identify the physicochemical properties of NPs that contribute to their bioactivity in order to adequately screen for their toxicity.

It has been postulated that dissociation of nanoparticle agglomerates may occur *in vivo* and that, following dissociation, smaller individual particles may then elicit differential effects as compared to the agglomerates. Along the same lines, it is thought that the type of material as well as the size of agglomerates determines the translocation and accumulation in exposed animal organs [27, 28]. Electron microscopy studies have confirmed a trend of carbon nanoparticle agglomerates to actually build larger units after deposition in the lungs and uptake in cells, which suggested that an enhanced translocation potential of individual nanoparticles derived from dissociation of those agglomerates should not be expected [29]. This conclusion is in accordance with theoretical considerations presented by Maier *et al.* [30] in a study on TiO_2 nanoparticles, in which the authors concluded that TiO_2 agglomerates do not dissociate following their contact with lung surfactants. They also concluded that the size of the formed agglomerate was expected to remain relatively stable once deposited within the respiratory tract,

10.1002/9783527692866.ch6, Downloaded from https://onlinelibrary.wiley.com/doi/10.1002/9783527692866.ch6 by NASA Shared Services Center (NSSC), Wiley Online Library on [19/05/2023]. See the Terms and Conditions (https://onlinelibrary.wiley.com/terms-and-conditions) on Wiley Online Library for rules of use; OA articles are governed by the applicable Creative Commons License

and this agglomerate size is likely to influence the resulting biological outcome [30]. However, Porter *et al*. [31] reported that an artificial lung lining fluid is a good dispersant of MWCNTs [31]. This result was confirmed with a pulmonary surfactant by Wang *et al.* [32]. Furthermore, Mercer *et al.* [33, 34] reported that inhaled small agglomerates of MWCNTs appeared to disperse over several months in the lung and that the singlets were translocated to extra-pulmonary organs. This information has been summarized by Castranova *et al.* [35].

6.2.4
Aspect Ratio Considerations

In addition to the type of carbon nanoparticles and their agglomeration state, another key determinant of nanoparticle bioactivity is the aspect ratio. CNTs are high-aspect-ratio nanomaterials (i.e., they are long and thin as opposed to short and thick) and thus have raised concerns that they may cause pulmonary responses similar to asbestos [16]. It is thought that changes in the length or thickness of CNTs may have a large impact on the activity of these particles.

Poland *et al.* [36] found a specific fiber-like effect of MWCNTs when injected intraperitoneally to mice. Each animal received a single injection of 100 $\mu g\ ml^{-1}$ of short or long amosite (asbestos) fibers or of short or long MWCNTs. Compared to the short fibers, long amosite fibers and long MWCNTs, respectively, induced a stronger inflammatory response and larger numbers of inflammatory granulomas [36]. Similarly, a different study found that long MWCNTs induced a more pronounced pro-fibrotic (mRNA expression of matrix metalloproteinase-8 and tissue inhibitor of metalloproteinase-1) and inflammatory (serum level of monocyte chemotactic protein-1) response compared with shorter and more agglomerated MWCNTs. This report also utilized Masson trichrome staining, which revealed epithelial cell hyperplasia upon exposure to the long MWCNTs [37].

A similar pro-fibrogenic effect of nanoparticles was observed with SWCNTs. Manke *et al.* [38] demonstrated that long SWCNTs were significantly more potent than short SWCNTs with respect to their ability to induce reactive oxygen species (ROS), collagen production, and transforming growth factor-beta (TGF-β) release in cultured human lung fibroblasts. The long SWCNTs were also more potent in inducing the fibrogenic and toxic effects *in vivo* when injected into the lungs of mice [38].

6.2.5
Surface Modifications

Surface modifications, such as changes in surface area, charge, coating, or reactivity, can greatly influence the bioactivity and/or toxic potential of carbon nanomaterials. These variations may be unintentional alterations due to differential production processes, or may be manipulated to intentionally alter the properties of nanoparticles. Surface charge and area can affect the cellular uptake of a particle, since it is the surface of the particle that will interact with cells and/or

10.1002/9783527692866.ch6 Downloaded from https://onlinelibrary.wiley.com/doi/10.1002/9783527692866.ch6 by NASA Shared Services Center (NSSC), Wiley Online Library on [19/05/2023]. See the Terms and Conditions (https://onlinelibrary.wiley.com/terms-and-conditions) on Wiley Online Library for rules of use; OA articles are governed by the applicable Creative Commons License

tissue. This notion has led to the idea that surface area should be considered as a dosing strategy rather than the mass per volume which is commonly used. Indeed, pulmonary responses have been shown to be different with changing the surface area of nanoparticles. A recent study by Shvedova *et al.* (2014) compared the pulmonary responses to SWCNTs by bolus dosing through pharyngeal aspiration and inhalation at 5 h per day for 4 days. Inhalation exposure to SWCNTs (more dispersed and thus greater structure surface) showed significantly greater inflammatory, fibrotic, and genotoxic effects than bolus pharyngeal aspiration (more agglomerated, less structure surface) [39]. The results of this study suggest that long-term pulmonary toxicity of SWCNTs, CNFs, and asbestos may be defined not only by their chemical composition but also by their specific surface area and the type of exposure.

Physical or chemical modifications to the surface of carbon nanoparticles, such as the addition of coatings or via carboxylation or amination (often termed "functionalization" of the NPs), are postulated to alter the biological effects of the NPs, and in some cases are thought to be able to reduce the toxicity of the particles. Continued efforts are going on to address this issue, while several studies have shed light on this approach for the design of carbon nanomaterials. For example, recent findings indicate that atomic layer deposition (ALD) and thin film coating of MWCNTs with Al_2O_3 reduces fibrosis in mice [40]. Similarly, carboxylation of SWCNTs and MWCNTs apparently makes them more vulnerable to oxidative destruction by peroxidases, thereby significantly decreasing their biopersistence and potentially making them less reactive [41, 42]. In addition, functionalization of MWCNTs via carboxylation has been shown to be less inflammatory and fibrogenic than without functionalization in mice exposed to the CNTs by aspiration [43, 44]. The data have also shown that amination of CNTs may lead to more adverse outcomes [43]. Collectively, these studies highlight the extent to which surface modifications may impact the bioactivity of carbon nanoparticles and provide critical insight into the utility of alternative design strategies for nanomaterial manufacturing.

6.3
Fate of Pulmonary Exposed Carbon Nanoparticles (Deposition, Distribution, Translocation, and Clearance)

6.3.1
Deposition and Distribution of Carbon Nanoparticles in the Lung

Deposition of inhaled nanoparticles on the airway walls occurs chiefly via diffusional displacement by the thermal motion of inhaled and exhaled air molecules in contact with the nanoparticles. Importantly, because of their geometry and hydrophobic surface, carbon nanoparticles have a tendency to form agglomerates with a bundle-like structure, thereby increasing in size from the nanoscale to the microscale. In contrast to microparticles, nanoparticles exhibit increased

10.1002/9783527692866.ch6, Downloaded from https://onlinelibrary.wiley.com/doi/10.1002/9783527692866.ch6 by NASA Shared Services Center (NSSC), Wiley Online Library on [19/05/2023]. See the Terms and Conditions (https://onlinelibrary.wiley.com/terms-and-conditions) on Wiley Online Library for rules of use; OA articles are governed by the applicable Creative Commons License

deposition as their size diminishes, with the deposition (nasal, tracheobronchial, and alveolus) being dependent on the aerodynamic diameter of the particles [45, 46]. Predicted fractional deposition of inhaled particles in the nasopharyngeal, tracheobronchial, and alveolar region of the human respiratory tract during nose breathing has also been reported [45].

Interestingly, yet not surprisingly, inhaled nanoscale and microscale particles end up differentially distributed in the lung. Mercer *et al.* [23] reported that pulmonary-aspirated large agglomerates of SWCNTs (~15 μm in diameter) remained in the alveolar airspaces of the terminal bronchioles and proximal alveoli, while well-dispersed SWCNTs (mean diameter of 0.69 μm) reached the distal alveoli, elicited minimal macrophage engulfment, and entered lung interstitium to induce interstitial fibrosis (Figure 6.2) [23]. Accordingly, it has been demonstrated that inhaled CNTs deposited in the bronchial and alveolar areas, but those deposited in the alveolar region were found to be smaller in size [49].

Pulmonary exposed CNTs can penetrate deep lung tissues, such as the interstitium, or translocate into pleura in a property-dependent manner [33, 47]. Accordingly, an interstitial penetration of nanoparticles and subsequent return onto airway epithelial cells has been reported [50]. In addition, pulmonary exposed MWCNTs have been shown to reach the subpleural area in mice after a single inhalation exposure of 30 mg m^{-3} for 6 h [51]. In this study, the CNTs were found embedded in the subpleural wall and within subpleural macrophages. The number and size of mononuclear cells located on the pleural surface also increased after 1 day of exposure, and subpleural fibrosis was observed 2 and 6 weeks after the exposure. Inhalation of CB nanoparticles or low-dose (1 mg m^{-3}) CNTs did not induce these effects. Other similar studies have also noted the presence of CNTs within the pleura (Figure 6.3), suggesting that the CNTs may have the ability to cause pleural fibrosis or mesothelioma, and highlighting the need for more long-term studies aimed at addressing this issue [33, 47, 51–53].

Mathematical models have been developed in an effort to predict particle deposition in the human airways. The model developed by the International Commission on Radiobiological Protection (ICRP) can be used to compute the proportions, by mass, of inhaled nanoparticles deposited in the airways of an individual breathing through the nose. Nanoparticles 1 nm in diameter are predicted to show ~90% deposition in the nasopharynx, 10% in the tracheobronchial tree, and 0% in the alveolar spaces; the corresponding proportions for 5-nm particles are 30%, 30%, and 30%, respectively, and for 20-nm particles, 15%, 15%, and 50%. With 20-nm particles, the distribution of deposition according to lung surface concentration indicates that alveolar space deposition is 100 times greater than nasopharyngeal deposition and 10 times greater than tracheobronchial deposition [54, 55].

Once deposited in the lungs, the nanoparticles may meet with different fates, in terms of cellular uptake and clearance. As such, endocytosis of nanoparticles has been extensively studied in various cell types. Endocytosis by airway epithelial

10.1002/9783527692866.ch6, Downloaded from https://onlinelibrary.wiley.com/doi/10.1002/9783527692866.ch6 by NASA Shared Services Center (NSSC), Wiley Online Library on [19/05/2022]. See the Terms and Conditions (https://onlinelibrary.wiley.com/terms-and-conditions) on Wiley Online Library for rules of use; OA articles are governed by the applicable Creative Commons License

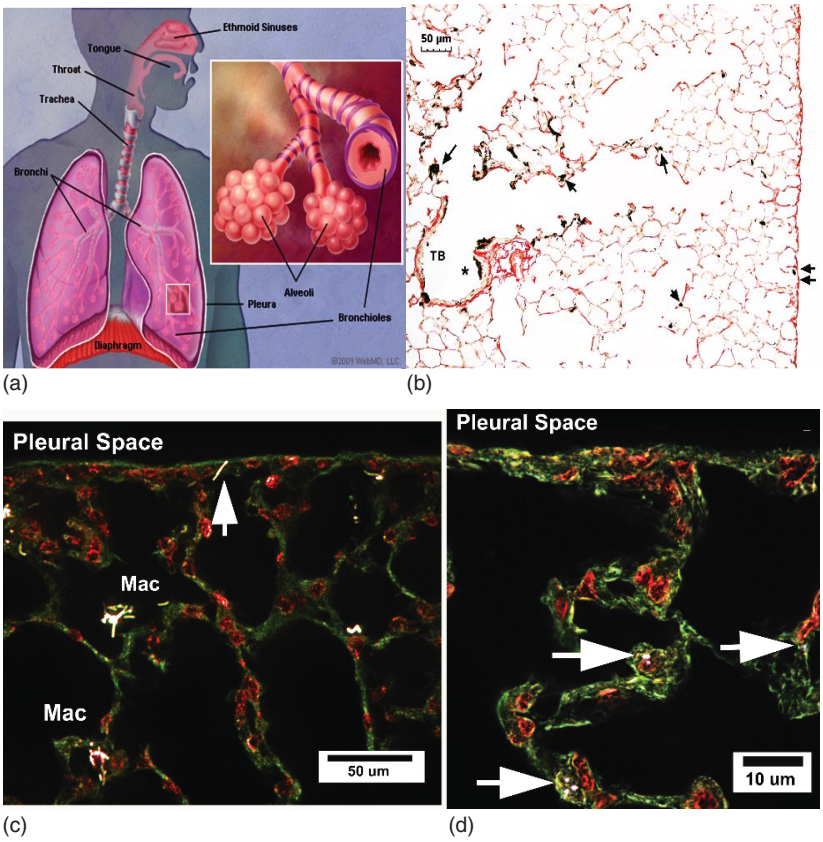

Figure 6.2 Pulmonary exposed MWCNT deposition. (a) Representative image of the lung (http://www.webmd.com/lung). (b) Light micrograph of MWCNT deposition in alveolar region of lungs. Sirius Red-stained micrograph shows the general deposition pattern of MWCNT (arrows) one day after 80 µg per mouse aspiration. A deposit of MWCNT on the epithelium of the terminal bronchiole near the transition between the airways and the alveolar region is indicated by single arrows. Smaller deposits near the subpleural tissue region are indicated by double arrows. Part (b) reprinted from [47]. (c, d) Enhanced dark-field images of the general distribution of CNTs as the bright, white structures in the lungs 7 days after aspiration (40 µg per mouse lung), while nuclei (red) and other tissues (green) produce a significantly duller image. (c) Arrow points to an individual MWCNT penetrating into the mesothelial cell layer forming the boundary between the alveolar tissues and pleural space. While alveolar macrophages are foci for MWCNTs, scattered/submicrometer MWCNT structures can be found in the alveolar interstitium throughout the section. (d) Mouse lung exposed to a highly dispersed preparation of SWCNTs (aspiration 10 µg per mouse lung, 7 days), for comparison. In the case of dispersed SWCNTs, the majority of CNT structures are rapidly incorporated into the alveolar interstitium (arrows). (Reprinted from [48].)

10.1002/9783527692866.ch6, Downloaded from https://onlinelibrary.wiley.com/doi/10.1002/9783527692866.ch6 by NASA Shared Services Center (NSSC), Wiley Online Library on [19/05/2023]. See the Terms and Conditions (https://onlinelibrary.wiley.com/terms-and-conditions) on Wiley Online Library for rules of use; OA articles are governed by the applicable Creative Commons License

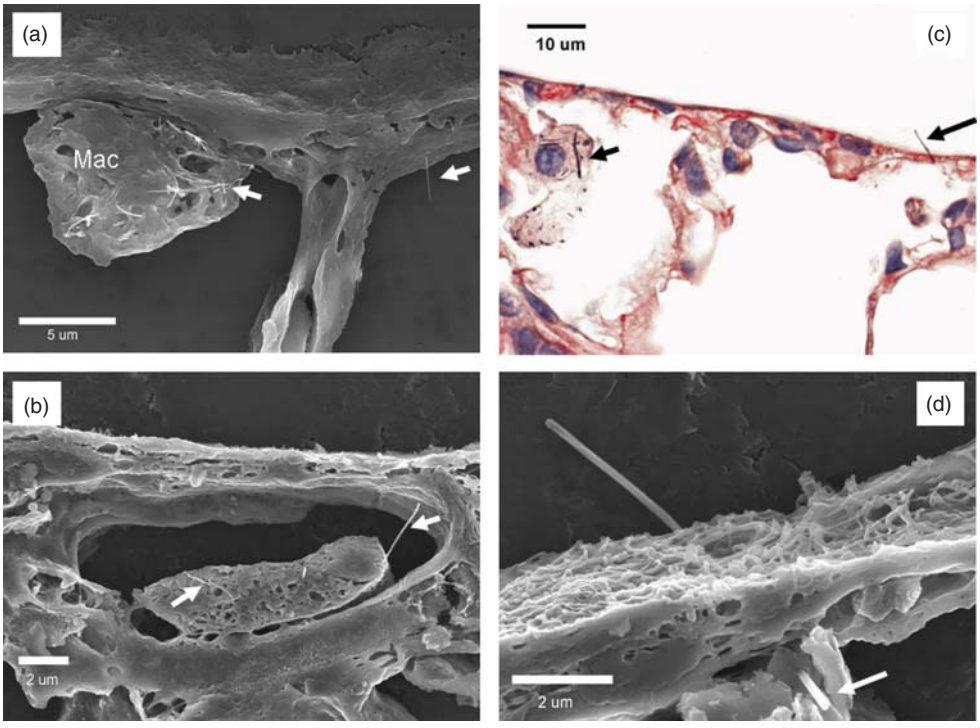

Figure 6.3 (a) Field-effect scanning electron microscopy image depicting an MWCNT-loaded alveolar macrophage and a single MWCNT fiber penetrating the alveolar epithelium into the subpleural tissues (80 μg dose, 28 days post aspiration). (b) Dilated subpleural lymphatic vessel containing a mononuclear inflammatory cell that is penetrated by several MWCNT fibers (80 μg dose, 56-day postaspiration). (c) An MWCNT penetrating the visceral pleura with a MWCNT-loaded alveolar macrophage visible in the left side of the micrograph (80 μg dose, 28 days post aspiration). (d) A single MWCNT penetrating from the subpleural tissue through the visceral pleura into the pleural space (80 μg dose, 56 days post aspiration). (Reprinted from [47].)

cells may occur at all three levels of the airway tree, providing nanoparticles direct entry into the blood and lymph and thereby allowing the particles to translocate to other parts of the body [45, 56, 57].

6.3.2 Translocation of Carbon Nanoparticles

Translocation into the epithelium and interstitium may allow nanoparticles to enter the blood and lymph, and thus distribute throughout the body [34, 50, 56–58]. Consistently, *in vivo* studies have shown effective translocation of ultrafine elemental carbon particles to the liver 1 day after inhalation exposure [57]. Translocation pathways include direct input into the blood compartment

10.1002/9783527692866.ch6, Downloaded from https://onlinelibrary.wiley.com/doi/10.1002/9783527692866.ch6 by NASA Shared Services Center (NSSC), Wiley Online Library on [19/05/2022]. See the Terms and Conditions (https://onlinelibrary.wiley.com/terms-and-conditions) on Wiley Online Library for rules of use; OA articles are governed by the applicable Creative Commons License

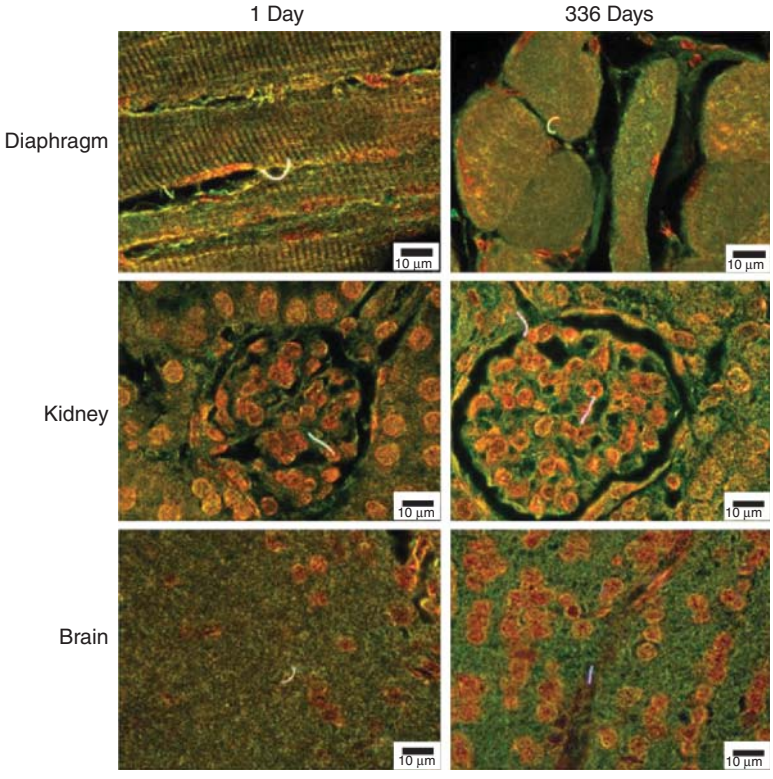

Figure 6.4 Enhanced dark-field images of MWCNT fibers in the diaphragm, kidney, and brain at 1 day and 336 days after inhalation exposure. MWCNT fibers in these figures are bright white, cell nuclei are brownish red, and other tissue elements are green. With rare exceptions, MWCNT fibers detected in extra-pulmonary organs were singlets. Normal (transmitted) light was blended into the fields and contrast-adjusted to make the tissue histology of the organs visible in these photographs. (Reprinted from [34].)

from ultrafine carbon particles deposited throughout the respiratory tract. Mercer *et al*. [33, 34] reported a qualitative study comparing the distribution of pulmonary exposed CNTs from 1 to 336 days after the termination of a 12-day inhalation exposure in order to determine whether there was a significant accumulation of CNTs in systemic tissues over time post exposure. The authors were able to detect the CNTs in lymph nodes, liver, kidney, heart, brain, chest wall, and diaphragm in as early as 1 day post exposure (1.089%) and noted a significant accumulation of CNTs in each of these organs at 336 days post exposure (7.337%), thus demonstrating the ability of the CNTs to translocate and accumulate systemically (Figures 6.4 and 6.5).

The report by Mercer *et al*. (2013) demonstrated the translocation and subsequent accumulation of a significant amount of CNTs within in the lymph nodes of exposed mice [34]. Likewise, a study conducted by Aiso *et al.* [59]

10.1002/9783527692866.ch6, Downloaded from https://onlinelibrary.wiley.com/doi/10.1002/9783527692866.ch6 by NASA Shared Services Center (NSSC), Wiley Online Library on [19/05/2023]. See the Terms and Conditions (https://onlinelibrary.wiley.com/terms-and-conditions) on Wiley Online Library for rules of use; OA articles are governed by the applicable Creative Commons License

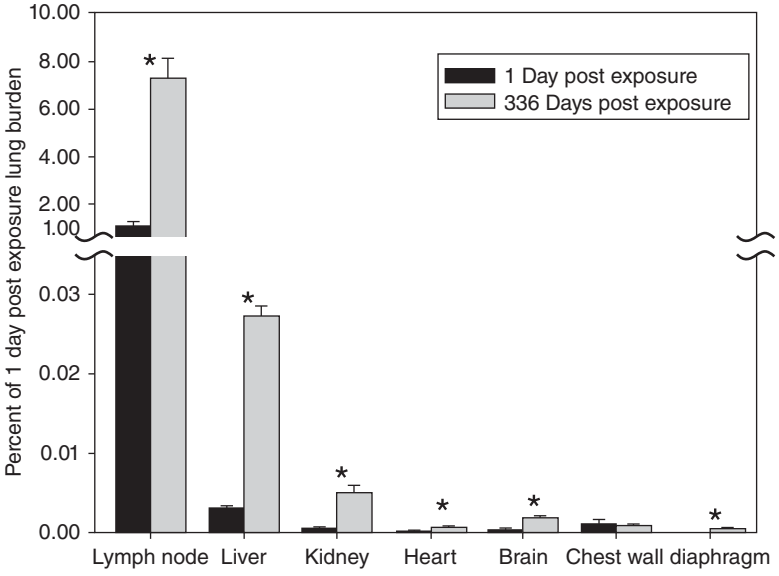

Figure 6.5 Percentage of the lung burden 1 day post exposure detected in tracheobronchial lymph nodes, extra-pulmonary organs, diaphragm, and chest wall. By 336 days post exposure, there was a sevenfold increase in MWCNTs in extra-pulmonary organs and diaphragm, compared to that measured at 1 day post exposure. Categories of extra-pulmonary organs are ordered relative to MWCNT concentration in the respective tissue. Asterisks indicate significant difference between day 1 and 336 days post exposure, $p < 0.05$. (Reprinted from [34].)

using a rat model showed that intratracheal instillation of MWCNTs led to translocation of the nanomaterials to the right and left posterior mediastinal lymph nodes, as well as some accumulation in the parathymic lymph nodes. The deposition of MWCNTs in the lymph nodes was found to increase gradually and dose-dependently with time [59].

Czarny *et al.* [60] reported a quantitative analysis of the tissue biodistribution of MWCNTs as a function of time. In this study, the authors utilized *in situ* ^{14}C-radiolabeled MWCNTs (20 μg per mouse) in combination with radioimaging of organ tissue sections for *ex vivo* electron microscopy analysis at regular intervals up to 1 year post exposure. It was observed that the MWCNTs were cleared slowly from the lungs. Translocation of MWCNTs increased over time, with MWCNTs being observed in numerous organs, notably the white pulp of the spleen and the bone marrow [60]. Another study evaluated the ability of MWCNTs to induce extra-pulmonary toxicities in rats following intratracheal instillation of two different types of MWCNTs into the lungs (0.2, 1, and 5 mg kg^{-1} body weight). Upon histopathological examination, it was found that each of the MWCNTs caused a dose-dependent toxic effect in the liver, including periportal lymphocytic infiltration, ballooning, foamy degeneration, and necrosis at each

10.1002/9783527692866.ch6, Downloaded from https://onlinelibrary.wiley.com/doi/10.1002/9783527692866.ch6 by NASA Shared Services Center (NSSC), Wiley Online Library on [19/05/2023]. See the Terms and Conditions (https://onlinelibrary.wiley.com/terms-and-conditions) on Wiley Online Library for rules of use; OA articles are governed by the applicable Creative Commons License

time point analyzed post exposure, while examination of the kidney revealed toxicity at the dose of 5 mg kg^{-1} at 1 month post instillation of both MWCNTs [61]. These results further demonstrate the ability of carbon nanoparticles to translocate to other organs and induce potentially toxic effects.

Translocation ability of inhaled nanoparticles also seems to be dependent on the type of particle analyzed as well as the amount of time until examination. In contrast to the aforementioned CNT studies, inhaled ultrafine carbon particles have been shown to be retained in the lung periphery and conducting airways without substantial systemic translocation or accumulation in the liver at 48 h post exposure [56]. In agreement with these findings, another report compared the bioaccumulation of iridium and carbon nanoparticles and found low but significant accumulation of two different sized iridium aggregates in the liver, spleen, kidneys, heart, and brain, as well as within soft tissue and bone. However, the authors observed only a very modest amount of carbon nanoparticle retention within these same organs at 24 h post exposure [28]

6.3.3
Clearance of Carbon Nanomaterials from the Lungs

Particles deposited in the airways are typically cleared by the mucociliary escalator transport that sweeps the particles up to the pharynx where they are subsequently swallowed, phagocytized by macrophages, or translocated through to the lymphatics. The main clearance mechanism of insoluble nanoparticles deposited in the tracheobronchial tree is via the mucocilary escalator and is rapid. Clearance of particles deposited in the alveolar spaces is via macrophage phagocytosis and is slower. The efficacy of this mechanism depends largely on the particle size and shape and whether agglomeration of the particles has occurred. As discussed earlier, several experimental studies in rodents have shown that well-dispersed carbon nanoparticles are poorly cleared by macrophage phagocytosis, the result being substantial accumulation of the CNTs within the alveoli and migration to the alveolar interstitium [23].

Lung retention or clearance of pulmonary-exposed solid particles depends primarily on the particle size and clearance capacity; compared to larger particles having the same chemical composition, inhaled nanoparticles show greater lung retention. After deposition in the lungs, nanoparticles can be cleared through several processes or may be redistributed to secondary target organs such as lymph nodes [34, 59, 62] and pleural sites [47, 51], and to distant organs [34, 63], which could be in a particle size-dependent manner [28]. As early as 1 day post exposure, the content of pulmonary exposed MWCNT fibers in the tracheobronchial lymph nodes was found principally in the form of singlets or a few fibers per MWCNT structure and accounted for 1.08% of the lung burden 1 day post exposure. MWCNT structures in tracheobronchial lymph nodes at 336 days included foci with dense accumulations with the content being substantially increased and equal to 7.34% of the lung burden 1 day post exposure (Figure 6.5, [34]). Deposition of intratracheally instilled MWCNT was greater in

10.1002/9783527692866.ch6, Downloaded from https://onlinelibrary.wiley.com/doi/10.1002/9783527692866.ch6 by NASA Shared Services Center (NSSC), Wiley Online Library on [19/05/2023]. See the Terms and Conditions (https://onlinelibrary.wiley.com/terms-and-conditions) on Wiley Online Library for rules of use; OA articles are governed by the applicable Creative Commons License

the posterior mediastinal lymph node than in the parathymic lymph node and was dose-dependent [59].

Carbon graphite whiskers (CGWs) were used in a 1-year inhalation study in male Wistar rats, and the biological effects were observed until the 1-year clearance period. Only ~30% of the total deposited CGWs were cleared during the 1-year postexposure period [64]. Several studies have sought to determine the retention time of carbon nanoparticles in the lungs. For example, Oyabu *et al.* [65] used rats that were exposed to well-dispersed MWCNTs for 4 weeks via whole-body inhalation at the exposure concentration of $0.37 \pm 0.18\,mg\,m^{-3}$. It was noted that ~70% of the exposed MWCNTs were single fibers with the geometric mean diameter and length of 63 nm and 1.1 μm, respectively. As determined by X-ray diffraction and elemental carbon analysis, the amounts of MWCNT deposited in the rat lungs at 3 days post inhalation were calculated to be 68 μg per lung (X-ray diffraction) and 76 μg per lung (elemental carbon analysis). Thus, the calculated deposition fractions were 18% and 20% in each analysis. After 3 months, the amount of retained MWCNT in the lungs sharply decreased with the calculated biological half-times of 51 days and 54 days, respectively [65]. In contrast, SWCNT aspiration studies carried out by Shvedova *et al.* (2014) showed that SWCNTs or CNFs can be seen in the lung at 1 year post exposure, suggesting the slow clearance of these particles from the lung [39]. Therefore, the low clearance rate and repeated exposure of carbon nanoparticles may result in significant pulmonary accumulation. Interestingly, Kagan *et al.* [66] recently demonstrated that SWCNTs may undergo oxidative biodegradation via superoxide/NO* → peroxynitrite-driven oxidative pathways, and thus may facilitate clearance of nanoparticles from the lung as macrophages "digest" the CNTs [66]. Consistently, several other studies have also reported that the process of enzymatic digestion of CNTs that may aid in their clearance from the lung [41, 42, 66]. Although these studies, and others, have shed some light on the mechanisms of clearance and retention of carbon nanomaterials within the lungs, the large number of different types of carbon nanoparticles, as well as the physicochemical properties of these NPs that can affect these processes, make it clear that additional studies are needed to fully understand the biological outcomes of the exposures.

6.4
Carbon Nanomaterial–Induced Lung Responses

6.4.1
Key/Specific Target Lung Cell Types of Pulmonary-Exposed Carbon Nanoparticles

Inflammation occurs as a result of an insult that activates the innate immune system, leading to the release of cytokines and chemokines, which makes inflammatory cells to respond to the insult or injury. These cells usually include neutrophils and macrophages, which can engulf foreign pathogens to aid in their

10.1002/9783527692866.ch6, Downloaded from https://onlinelibrary.wiley.com/doi/10.1002/9783527692866.ch6 by NASA Shared Services Center (NSSC), Wiley Online Library on [19/05/2023]. See the Terms and Conditions (https://onlinelibrary.wiley.com/terms-and-conditions) on Wiley Online Library for rules of use; OA articles are governed by the applicable Creative Commons License

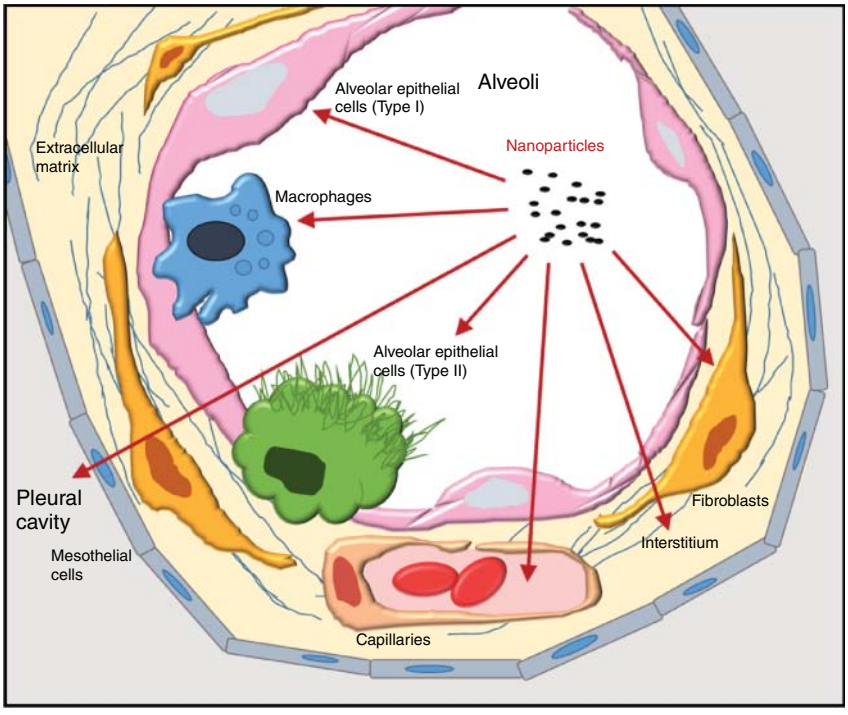

Figure 6.6 Lung cells potentially affected by inhalation of nanoparticles.

clearance. This innate inflammatory response helps to induce activation of the adaptive/humoral response mediated by T cells and B cells, which coordinate the production of antibodies to promote the clearance of foreign pathogens. For carbon nanoparticles, as discussed earlier, the main route of exposure for humans is via inhalation, often resulting in a rapid innate immune response within the lung to recruit phagocytic cells to clear the material. Thus, the major cell types involved in the immune response to these particles generally include alveolar macrophages and, to some degree, neutrophils [62, 67]. Other lung cells are also affected, primarily alveolar epithelial cells, fibroblasts, and possibly pleural mesothelial cells (Figure 6.6). These cells types are able to release various inflammatory mediators, and aberrant stimulation of these cell types is believed to contribute to the development of diseases such as fibrosis or cancer [62, 68].

In terms of cellular interactions with carbon nanoparticles, again, it seems that the particle type and size may play a role. For example, in one study, three different MWCNTs (one short (850 nm) and tangled, and two longer (4 and 5.7 μm) and thicker) were intratracheally instilled into mice and were analyzed for cellular interactions 1, 3, and 28 days after instillation. TEM analysis revealed that all three CNTs were taken up either by a diffusion mechanism or via

10.1002/9783527692866.ch6, Downloaded from https://onlinelibrary.wiley.com/doi/10.1002/9783527692866.ch6 by NASA Shared Services Center (NSSC), Wiley Online Library on [19/05/2023]. See the Terms and Conditions (https://onlinelibrary.wiley.com/terms-and-conditions) on Wiley Online Library for rules of use; OA articles are governed by the applicable Creative Commons License

endocytosis, and subsequently agglomerated within vesicles in macrophages. However, at 28 days post exposure, the longer and thicker MWCNTs were able to more efficiently escape the vesicular enclosures in macrophages compared to the smaller CNTs, and resulted in more severe eosinophil influx and incidence of eosinophilic crystalline pneumonia [69]. Thus, the target cell types as well as the responses of those cells are likely to differ depending on the characteristics of the nanoparticle.

6.4.2 Lung Inflammation

A large percent of human exposures to respirable carbon nanomaterials is thought to occur as a result of the manufacturing process in an occupational setting, and, as such, several studies have been conducted in an effort to determine whether these working conditions cause lung inflammation or disease. Consistent with this notion, nano-scaled CB particle exposure was found to be the likely cause for reduced lung function and pro-inflammatory cytokine secretion in CB workers, and animals exposed to aerosolized CB particles showed alveolar wall thickening and a significant increase of inflammatory cells in lung tissues after CB exposure [70, 71].

Another study conducted by Lee *et al*. [72] investigated the health effects of MWCNTs in a manufacturer's facility, which included an assessment of the personal and area-specific exposure levels to MWCNTs, as well as exhaled breath condensates (EBCs) and lung function tests from the manufacturing and office workers at the facility. Exposure levels to elemental carbon were found to be $6.2-9.3\,\mathrm{mg\,m^{-3}}$ in the personal samplings and $5.5-7.3\,\mathrm{mg\,m^{-3}}$ in the area samplings. All workers were found to have normal blood chemistry readings as well as normal lung function parameters; however, the EBC analysis revealed increased levels of malondialdehyde (MDA) and 4-hydroxy-2-hexenal (4-HHE), which are markers of oxidative stress and lipid peroxidation, respectively, in the MWCNT manufacturing workers compared to the office workers [72].

Animal models have also been used in an effort to examine the lung inflammatory responses to carbon nanoparticles. Several studies have observed significant lung inflammation and damage at 1 day post MWCNT exposure in rodent models [33, 52]. Interestingly, numerous studies have noted little or transient inflammatory responses but with rapid and persistent interstitial fibrosis or granulomas at the sites of deposition of nanoparticle agglomerates [2, 23, 25, 48, 52, 59, 73, 74]. Similarly, accumulating data also reveal that pulmonary exposure of animals to carbon nanomaterials leads to acute neutrophilic inflammation [24, 75]. Collectively, this would suggest that following exposure to carbon nanoparticles, acute and transient inflammation would primarily serve to recruit macrophages and neutrophils for phagocytosis of the particles, which can ultimately lead to granuloma formation and fibrosis.

Consistently, several studies have observed the formation of granulomas in response to carbon nanomaterials. Warheit *et al*. [76] noted that agglomerated

10.1002/9783527692866.ch6, Downloaded from https://onlinelibrary.wiley.com/doi/10.1002/9783527692866.ch6 by NASA Shared Services Center (NSSC), Wiley Online Library on [19/05/2022]. See the Terms and Conditions (https://onlinelibrary.wiley.com/terms-and-conditions) on Wiley Online Library for rules of use; OA articles are governed by the applicable Creative Commons License

SWCNTs (with or without metallic residues) induced an inflammatory response with granulomas surrounding the nanotubes, indicating pulmonary toxicity [76]. Similar granulomas were found in rats intratracheally instilled with SWCNTs, although the inflammation resolved within 3 months [23, 25]. Another 90-day study reported granulomatous inflammation, with macrophage and T-cell infiltration, that persisted up to 90 days, and the authors noted a marked elevation in osteopontin, metalloproteinases, and cell adhesion molecules in granulomatous foci, as well as alveolar macrophages from bronchoalveolar lavage [77].

6.4.3 Immune Response

In terms of immune response, in addition to inflammation, CNT exposure may actually enhance allergic asthma induction. For instance, Inoue *et al.* [78] reported that MWCNTs administered intratracheally significantly increased ovalbumin-induced T-lymphocyte proliferation and amplified lung Th_2 cytokines and chemokines as compared with ovalbumin exposure alone [78]. Work by Park *et al*. showed that MWCNT instillation activated alveolar macrophages, resulting in the attraction of immune cells to the BAL fluid. Pro-inflammatory cytokines (IL-1, TNF-α, and IL-6), Th1-type cytokines (IL-12 and IFN-γ), and Th2-type cytokines (IL-4, IL-5, and IL-10) were increased both in BAL fluids and in blood. Differentiation of CD4+ T cell to Th1 cells and Th2 cells were triggered by IL-12 and IL-4, respectively. The elevated numbers of B cells activated by IL-10 were then involved in the production of IgE. This combination of responses may have caused the allergic reactions observed in the mice treated with MWCNTs [79]. Another study determined that exposure of mice to ovalbumin before inhalation of MWCNTs caused significant airway fibrosis in an allergic asthma mouse model, whereas ovalbumin or MWCNTs alone did not significantly increase airway fibrosis in these mice [80].

Similarly, Ronzani *et al*. (2014) investigated the effect of MWCNTs on the immune responses and reported that MWCNT exposure resulted in the aggravation of airway inflammation and remodeling and in increased production of epithelium-derived innate cytokines in a mouse model of asthma. In this study, using a common asthma-causing allergen, namely the house dust mite (HDM), the authors examined common markers of asthma such as the production of the innate cytokines, thymic stromal lymphopoietin (TSLP), IL-25, IL-33, and GM-CSF, as well as the influx of macrophages, eosinophils, and neutrophils, and the production of collagen, transforming growth factor beta 1 (TGF-β1), and mucus. BALB/cByJ mice were exposed by intranasal instillation to HDM + MWCNT and compared with those exposed to HDM alone. The results showed that HDM-treated mice exhibited specific IgG1 in serum and inflammatory cell infiltration as well as increased Th2 cytokine production, mucus hyperproduction, and collagen deposition in the airways when compared to naïve animals. In mice exposed to HDM + MWCNT, the levels of total IgG1, HDM-specific IgG1, IL-13, eotaxin, TARC influx of macrophages, eosinophils, and neutrophils, and production of

10.1002/9783527692866.ch6, Downloaded from https://onlinelibrary.wiley.com/doi/10.1002/9783527692866.ch6 by NASA Shared Services Center (NSSC), Wiley Online Library on [19/05/2023]. See the Terms and Conditions (https://onlinelibrary.wiley.com/terms-and-conditions) on Wiley Online Library for rules of use; OA articles are governed by the applicable Creative Commons License

collagen, TGF-β1, and mucus were dose-dependently increased compared to those exposed to HDM alone [82]. These results demonstrate that pulmonary exposed MWCNTs increase immune responses in a dose-dependent manner, as well as airway allergic inflammation and remodeling induced by HDM in the mouse.

Overall, there is limited information on pulmonary exposed, carbon nanomaterial–induced systemic immune responses. It is unknown whether CNTs will cause or exacerbate asthma in humans.

6.4.4 Fibrosis

Lung fibrosis has been observed, in varying degrees of severity, in a number of rodent lung models exposed to carbon nanoparticles. Fibrosis is primarily characterized by two main pathological features, that is, excessive accumulation of extracellular matrix proteins such as collagen, and the uncontrolled proliferation of fibroblasts, which together lead to remodeling of the lung architecture [82]. Given the fact that once fibrosis develops there are currently no effective therapeutic treatment options, it is important to consider the fibrogenic potential of all emerging nanotechnologies.

In the case of CNTs, numerous studies have been conducted to determine the fibrogenicity of these nanomaterials. Intratracheal instillation or pharyngeal aspiration of CNT suspensions, which agglomerate into micrometer-sized bundles in aqueous media, stimulates the formation of inflammatory foci known as granulomas within the lung parenchyma. These granulomas, containing fibrotic collagen, have been reported in mice or rats within days of exposure [2, 25, 73, 75, 76]. Interestingly, well-dispersed CNTs resulted in less deposition in the large airways and fewer granulomas. However, more dispersed CNTs exhibited augmented deposition in the deep lung, their migration to the alveolar interstitium, and significantly increased alveolar interstitial fibrosis [23, 25].

Short-term exposure to double-walled CNTs produced dose-dependent pulmonary inflammation, cytotoxicity, and decreased the integrity of blood–gas barrier in the lung, in addition to inducing significant alveolitis and fibrosis in mice at 7 and 56 days post exposure [83]. When considering more long-term effects of carbon nanoparticles, Shvedova *et al.* (2014) recently examined the effects of SWCNTs, CNFs, and asbestos on lung pathology 1 year after a bolus dose of particles via pharyngeal aspiration or through inhalation at 5 h per day for 4 days. The authors could observe substantial levels of particles in the lungs 1 year post exposure, with some in the lymphatic system. Additionally, each of the particles induced chronic bronchopneumonia and lymphadenitis, accompanied by pulmonary fibrosis. On an equal mass basis, SWCNTs were the most fibrogenic of all of the particles tested. Inhalation of SWCNTs was also found to be fibrotic, inflammatory, and genotoxic [39].

Another 13-week study in a rat model used whole-body inhalation to MWCNTs at the concentrations of 0, 0.2, 1, and 5 mg m^{-3} with mass median aerodynamic

10.1002/9783527692866.ch6, Downloaded from https://onlinelibrary.wiley.com/doi/10.1002/9783527692866.ch6 by NASA Shared Services Center (NSSC), Wiley Online Library on [19/05/2023]. See the Terms and Conditions (https://onlinelibrary.wiley.com/terms-and-conditions) on Wiley Online Library for rules of use; OA articles are governed by the applicable Creative Commons License

diameter of 1.4–1.6 μm, mean width of 94.1–98.0 nm, and mean length of 5.53–6.19 μm, respectively [74]. They observed that inflammatory parameters increased in a concentration-dependent manner from 0.2 mg m^{-3}. Granulomatous changes in the lung were induced at 1 and 5 mg m^{-3} in female rats, and at even a lower dose of 0.2 mg m^{-3} in males. Focal fibrosis of the alveolar wall was observed in both sexes at 1 mg m^{-3} or higher. Moreover, inflammatory infiltration in the visceral pleural and subpleural areas was induced only at 5 mg m^{-3}.

In terms of the mechanism of carbon nanoparticle–induced fibrosis, several theories have been proposed. For example, these bioeffects could be ROS-related. In $ApoE^{-/-}$ transgenic mice, which is a common model for atherosclerosis, examination of the aorta after 7, 28, and 60 days showed mitochondrial DNA damage and oxidative stress after a single intratracheal instillation of SWCNTs [84, 85]. Shvedova *et al*. also recently reported that lipid-derived free radicals contribute to tissue damage induced by SWCNTs, not only in the lungs but also in other organs [86]. Others have postulated, based on the evidence that well-dispersed CNTs can penetrate the alveolar epithelial barrier and enter the interstitium, that carbon nanoparticles may have a direct effect on fibroblasts. Such migration of dispersed SWCNTs or MWCNTs has been reported [23, 33, 34]. As the main producers of collagen, aberrant stimulation of fibroblasts by carbon nanomaterials could induce a fibrotic response. Indeed, *in vitro* analysis using individual lung cell types support the notion that CNTs can directly stimulate fibroblast cell proliferation and collagen production, a hallmark of fibrogenesis [32]. It is also noteworthy, as previously mentioned, that numerous studies have noted little or only transient inflammatory responses to CNTs, but with rapid onset of interstitial fibrosis or granulomas at the sites of nanoparticle deposition [2, 23–25, 48, 52, 59, 73, 74]. This may also support the idea that CNT-induced fibrosis occurs, at least in large part, as a result of the direct stimulation of fibroblasts by these materials without an overt inflammatory response *in vivo* [23, 73].

6.4.5 Genotoxicity

Several studies have observed some degree of genotoxicity in response to carbon nanomaterials, primarily CB. Kyjovska *et al*. [87] reported statistically significant increases in DNA strand breaks in mouse lung BAL cells after a single exposure to CB at the doses of 0.67–6 mg per mouse at 1–28 days post exposure. This DNA damage was found to be primary genotoxicity, which occurred in the absence of inflammation and cell damage, indicating that inflammation is not required for the genotoxic effects of CB [87]. Similarly, another study found that deposition of CB nanoparticles in the lung induced persistent inflammatory and genotoxic effects in mice, not only in the lung but also in other organs such as the liver [88]. Interestingly, this same group found that CB had no effect on cardiac cell gene expression [89]. Collectively, these results suggest that carbon nanoparticles may

10.1002/9783527692866.ch6, Downloaded from https://onlinelibrary.wiley.com/doi/10.1002/9783527692866.ch6 by NASA Shared Services Center (NSSC), Wiley Online Library on [19/05/2023]. See the Terms and Conditions (https://onlinelibrary.wiley.com/terms-and-conditions) on Wiley Online Library for rules of use; OA articles are governed by the applicable Creative Commons License

induce genotoxicity and highlight the need for additional studies to shed light on this notion.

6.4.6 Cancer

The similarities of CNTs and nanofibers to asbestos in terms of their fiber-like morphology, durability, and high aspect ratio present new challenges to assess, understand, and manage potential adverse health effects caused by human exposure. As discussed throughout this chapter, substantial evidence from mammalian toxicity studies indicates that inhalation exposure to this class of engineered nanoparticles can cause adverse pulmonary effects. Thus, the ability of CNTs to induce cancer has also been the subject of frequent studies.

In the case of CNTs, studies have found that these particles demonstrate carcinogenic characteristics in rodent models. By utilizing a two-stage initiation/promotion protocol *in vivo* to determine carcinogenic potential of CNTs, Sargent *et al*. [68] reported for the first time that some MWCNT exposures, but not vehicle control, promoted the growth and neoplastic progression of initiated lung cells in B6C3F1 mice that received a single intraperitoneal (IP) injection of the initiator methylcholanthrene (MCA, 10 μg g^{-1} BW). IP injection of MCA was followed 1 week later by inhalation of MWCNTs (5 mg m^{-3}, 5 h per day, 5 days per week) or filtered air (controls) for a total of 15 days (MWCNT lung burden of 31.2 μg per mouse approximates feasible human occupational exposures). At 17 months post treatment, 23% of the filtered air controls and 26.5% of the MWCNT-exposed, 51.9% of the MCA-exposed, and 91% of the MCA/MWCNT-exposed mice had lung tumors. Furthermore, 62% of the mice exposed to MCA followed by MWCNT had bronchiolo-alveolar adenocarcinomas compared to 13% of the mice that received filtered air, 22% of the MCA-exposed, or 14% of the MWCNT alone-exposed animals [68]. Consistently, chronic *in vitro* studies using cultured human lung epithelial or mesothelial cells support this finding, with results demonstrating that CNTs can stimulate cell proliferation, migration/invasion, and colony formation, and that SWCNT-transformed human bronchial epithelial cells (BEAS-2B) can form tumors in mice [90].

Other studies have also detected the carcinogenic potential of CNTs. For example, MWCNTs or crocidolite (asbestos) fibers administered as a single intraperitoneal injection in mice induced mesothelioma in 15.8% (3/19) and 31.6% (6/19) of $p53^{+/-}$ animals, respectively [91]. In contrast, no cases of mesothelioma were seen among $p53^{+/-}$ mice exposed to fullerene nanoparticles or unexposed $p53^{+/-}$ mice [68, 91]. Moreover, Shvedova *et al*. [92] reported that exposure to SWCNTs induced recruitment and accumulation of lung-associated, myeloid-derived suppressor cells (MDSC) and MDSC-derived production of

10.1002/9783527692866.ch6, Downloaded from https://onlinelibrary.wiley.com/doi/10.1002/9783527692866.ch6 by NASA Shared Services Center (NSSC), Wiley Online Library on [19/05/2023]. See the Terms and Conditions (https://onlinelibrary.wiley.com/terms-and-conditions) on Wiley Online Library for rules of use; OA articles are governed by the applicable Creative Commons License

TGF-β, leading to increased tumor burden in the lung. The authors concluded that pulmonary exposure to SWCNTs aids in the formation of a niche that supports lung carcinoma *in vivo* via induction of TGF-β by SWCNT-attracted and presensitized lung-associated MDSC [92]. This group also demonstrated that SWCNTs and CNFs, but not asbestos, increased the incidence of K-ras oncogene mutations in the lung of mice 1 year post exposure; however, no increased lung tumor incidence occurred in this time [39].

As previously mentioned, the similar morphologies of CNTs and asbestos leave many wondering about the potential for CNTs to induce asbestos-like health hazards such as pleural inflammation, fibrosis, and mesothelioma. Length-dependent pathogenicity is a feature of asbestos. A general mechanism for fiber pathogenicity in the pleural cavity is related to the size-restricted clearance mechanisms from the pleural space and the subsequent selective retention of long fibers [93]. This mechanism is independent of chemical composition, other than how chemical composition affects biopersistence, and has been validated by the fact that a number of different fiber types, including asbestos, CNTs, and a number of nanowires, all generate a length-dependent inflammatory response after direct injection into the pleural or peritoneal cavities [36, 94, 95]. The results presented by Murphy *et al*. [94] support a length-dependent pathogenicity of CNTs in the lungs and pleural space following airspace deposition, similar to asbestos. These data support the contention that long CNTs reach the pleura from the airspaces and that they are retained at the parietal pleura and cause inflammation and lesion development. The parietal pleura is the site of origin of mesothelioma, and inflammation is considered to be a process involved in asbestos-induced carcinogenesis. Thus, these data support the assertion that CNTs may pose an asbestos-like mesothelioma hazard [94], indicating that this should be explored in greater detail. Indeed, the study mentioned above demonstrated that MWCNTs administered as a single intraperitoneal injection in mice induced mesothelioma in 15.8% (3/19) and 31.6% (6/19) of $p53^{+/-}$ animals, respectively [68, 91]. The International Agency for Research of Cancer has classified Mitsui-7 MWCNT as class 2B, that is, a possible human carcinogen [96].

Additional studies have been carried out to evaluate the carcinogenicity of other carbon nanomaterials such as CB. Carbon black is widely used in numerous industrial applications, including the production of rubber, tires, paints, toners, and printing inks, and this particle has been classified as a possible human carcinogen (group 2B) by the International Agency for Research on Cancer [96, 97]. In addition, there is evidence for carcinogenicity in rats, together with supporting evidence from human data of structurally related substances, and thus the European Union (EU) criteria for category 2 of carcinogenic substances appear to be fulfilled for bio-durable nanoparticles consisting of matter without known significant specific toxicity [98, 99]. Using rat models, it has been estimated that airborne UFCB concentrations of approximately $0.07-0.3\ \mathrm{mg\ m^{-3}}$ over a lifetime of working conditions are associated with a 0.1% excess risk of lung cancer [100].

10.1002/9783527692866.ch6, Downloaded from https://onlinelibrary.wiley.com/doi/10.1002/9783527692866.ch6 by NASA Shared Services Center (NSSC), Wiley Online Library on [19/05/2022]. See the Terms and Conditions (https://onlinelibrary.wiley.com/terms-and-conditions) on Wiley Online Library for rules of use; OA articles are governed by the applicable Creative Commons License

6.4.7
Cardiovascular Effects Following Pulmonary Exposure of Carbon Nanomaterials

Induction of the acute-phase response following pulmonary deposition of different kinds of particles, including carbon nanoparticles, is closely linked to risks for cardiovascular diseases, as shown in both epidemiological and animal studies [101]. Blood levels of acute-phase proteins, such as C-reactive protein and serum amyloid A, have been found to be independent predictors of the risk of cardiovascular disease in prospective epidemiological studies [102]. Indeed, inhalation and instillation of numerous nanoparticles, including SWCNTs, MWCNTs, and CB, have been shown to induce pulmonary acute-phase responses [67, 103–109]. In addition, inhalation of MWCNT has been shown to depress the ability of coronary arterioles to respond to dilators [63]. Taken together the studies reviewed herein, it is plausible that exposure to carbon nanoparticles increases the risk of cardiovascular disease.

6.5
Summary

Nanotechnology is a fast growing field that has developed a demand for carbon nanomaterials with novel physicochemical properties for a broad array of applications. Knowledge of their unique bioeffects once exposed to the lung are still limited and critically needed to ensure safe implementation of nanotechnology for utility within the medical field, as well as standards for unintentional pulmonary exposure. Available data from the literature of pertinent pulmonary response studies of carbon nanomaterials suggest that inhaled nano-scaled carbon materials can deposit deep in the lung tissue and distribute into the alveolar interstitium where micrometer-sized particles generally cannot reach. They have also been found in the pleural area, similar to asbestos, and at extra-pulmonary locations but with low translocation rate from the lung. The degree of toxic effects, such as inflammation, lung cell cytotoxicity and genotoxicity, lung fibrosis, and carcinogenic potential, seem to be largely physicochemical property-dependent, highlighting the ever-growing challenge of thoroughly assessing the potential hazards of this expanding area of nanotechnology. A summary of pulmonary toxicology studies for carbonaceous nanoparticles is given in Table 6.1.

Disclaimer

The findings and conclusions in this report are those of the authors and do not necessarily represent the views of the National Institute for Occupational Safety and Health.

10.1002/9783527692866.ch6, Downloaded from https://onlinelibrary.wiley.com/doi/10.1002/9783527692866.ch6 by NASA Shared Services Center (NSSC), Wiley Online Library on [19/05/2023]. See the Terms and Conditions (https://onlinelibrary.wiley.com/terms-and-conditions) on Wiley Online Library for rules of use; OA articles are governed by the applicable Creative Commons License

Table 6.1 Summary of studies on pulmonary effects of carbon nanomaterials.

Type of carbon nanomaterial	Sources	Animal model	Exposure dose/method	Exposure time	Major findings	References
Carbon black	Evonik Industries, Hanau, Germany	Female BALB/c mice	Single or 8 oropharyngeal aspirations at week 1–3, 5, 7, 9, 11, and 12 using 7 μg Printex 90, 7 μg DQ12 quartz (as a positive control)	2-Day and 3-month post-exposure analysis	Multiple CBNP applications produced: • Reduced lung function • Collagen accumulation • Elevated phospholipid levels in BALF, and a massive infiltration of macrophages • Type II pneumocyte mRNA expression of antioxidative enzymes remained unchanged throughout the subchronic experiment, but showed a significant decrease in interleukin (IL)-6Rα mRNA expression	[70]
SWCNT	CNI, Inc.	C57BL/6J mice	Single pharyngeal aspiration of 0, 10, 20, and 40 μg per mouse	1, 3, 7, 28, and 60 days post-exposure analysis	• Robust but acute inflammation with early onset, yet progressive, fibrosis and granulomas • Interstitial fibrosis and alveolar wall thickening	[23, 25, 32, 110]
SWCNT (effect of length)	Cheap Tubes Inc., Brattleboro, VT, USA	C57BL/6J mice	Single pharyngeal aspiration 40 μg per mouse	90 Days post-exposure analysis	• Long SWCNTs were significantly more potent than short SWCNTs at inducing fibrogenesis	[38]

(*continued overleaf*)

10.1002/9783527692866.ch6, Downloaded from https://onlinelibrary.wiley.com/doi/10.1002/9783527692866.ch6 by NASA Shared Services Center (NSSC), Wiley Online Library on [19/05/2023]. See the Terms and Conditions (https://onlinelibrary.wiley.com/terms-and-conditions) on Wiley Online Library for rules of use; OA articles are governed by the applicable Creative Commons License

Table 6.1 (*Continued*)

Type of carbon nanomaterial	Sources	Animal model	Exposure dose/method	Exposure time	Major findings	References
MWCNT	Mitsui and Co., Japan	C57BL/6J mice	Single pharyngeal aspiration 0, 10, 40, and 80 μg per mouse lung	1, 7, 28, and 56 Days post-exposure analysis	• Pulmonary inflammation was dose-dependent and peaked at 7 days post exposure • Rapid development of pulmonary fibrosis by 7 days post exposure • Granulomatous inflammation persisted throughout the 56-day post-exposure period • MWCNT can reach the pleura after pulmonary exposure • Lung burden was predominately within alveolar macrophages (~8% delivery to the alveolar septa; and a smaller burden in subpleural tissues) • Average thickness of connective tissue in the alveolar septa increased 45% in the 40 μg and 73% in the 80 μg exposure groups	[48, 52]
MWCNT	Hodogaya Chemical Company (MWNT-7, lot #061220-31)	C57BL/6J	Inhalation 5 mg m^{-3} aerosol for 5 h per day	(Four times per week for 3 weeks, lung burden = 28.1 μg per lung)	• Dose-dependent pulmonary inflammation • Rapid development of pulmonary fibrosis • Transported to the parietal pleura, the respiratory musculature, liver, kidney, heart, and brain in a singlet form and accumulate with time following exposure • The tracheobronchial lymph nodes contain high levels of MWCNT following exposure and further accumulate over nearly a year	[33, 34]

10.1002/9783527692866.ch6, Downloaded from https://onlinelibrary.wiley.com/doi/10.1002/9783527692866.ch6 by NASA Shared Services Center (NSSC), Wiley Online Library on [19/05/2023]. See the Terms and Conditions (https://onlinelibrary.wiley.com/terms-and-conditions) on Wiley Online Library for rules of use; OA articles are governed by the applicable Creative Commons License

MWCNT	Mitsui and Co., Japan	B6C3F1 mice	Inhalation of 5 mg m^{-3}, 5 h per day, 5 days per week for 15 days (lung burden of 31.2 μg per mouse) 1 week after i.p. initiator methylcholanthrene (10 μg g^{-1} BW; i.p.)	17 months post-treatment analysis	• MWCNT exposures promote the growth and neoplastic progression of initiated lung cells in B6C3F1 mice	[68]
MWCNT	Helix Material Solutions, Inc. (Richardson, TX)	C57BL/6J mice and ovalbumin-sensitized mice	Aerosol (100 mg m^{-3}) or saline aerosol for 6 h	1 and 14 days post-inhalation analysis	• Airway fibrosis which required preexisting inflammation	[80]
Functionalized MWCNT: COOH; PEG; NH_2; sidewall NH_2; PEI-modified	Raw CNTs from Cheap Tubes, Inc., Own modified	C57BL/6 mice	2 mg kg^{-1} Body weight	21 Days	• Fibrogenic effects in the following sequence: Anionic (COOH and PEG) < pristine ≈ neutral < strong cationic (PEI)	[43]
MWCNT: COOH	Nanostructured and Amorphous Materials, Inc., Houston, TX. Own modified MWCNT-COOH	C57BL/6 mice	Single pharyngeal aspiration of 0, 2.5, 10, or 40 μg per mouse	1, 7, and 56 Days post-exposure analysis	• Functionalized COOH significantly reduced inflammation and lung fibrosis	[44]

(*continued overleaf*)

10.1002/9783527692866.ch6, Downloaded from https://onlinelibrary.wiley.com/doi/10.1002/9783527692866.ch6 by NASA Shared Services Center (NSSC), Wiley Online Library on [19/05/2023]. See the Terms and Conditions (https://onlinelibrary.wiley.com/terms-and-conditions) on Wiley Online Library for rules of use; OA articles are governed by the applicable Creative Commons License

Table 6.1 (*Continued*)

Type of carbon nanomaterial	Sources	Animal model	Exposure dose/method	Exposure time	Major findings	References
Fullerene	Henan University, China	Sprague–Dawley (SD) rats	Intratracheal instillation of 3.7×10^7 Bq ^{99m}Tc-C_{60}(OH)x and $Na^{99m}TcO_4$ in 0.3 ml volume		• Large proportion of the ^{99m}Tc-c060(OH)x was retained in the lung • Transient penetration of the alveolar–capillary barrier by the ^{99m}Tc-c060(OH)x with some translocation into the blood • Uptakes in the liver, bone, and spleen	[12, 111]
Graphene	Cabot	C57BL/6 mice	Single pharyngeal aspiration of 4 or 40 μg three different sized graphene (Gr1, Gr5, or Gr20)/mouse	4 h (day 0), 1, 7, and 28 days postexposure	• Acute inflammation and lung damage • Larger Gr particles appeared to produce more toxicity at the early time points post exposure when compared to controls	[112]

10.1002/9783527692866.ch6, Downloaded from https://onlinelibrary.wiley.com/doi/10.1002/9783527692866.ch6 by NASA Shared Services Center (NSSC), Wiley Online Library on [19/05/2023]. See the Terms and Conditions (https://onlinelibrary.wiley.com/terms-and-conditions) on Wiley Online Library for rules of use; OA articles are governed by the applicable Creative Commons License

References

1. Oberdorster, G. (2010) *J. Intern. Med.*, **267**, 89.
2. Lam, C.W., James, J.T., McCluskey, R., and Hunter, R.L. (2004) *Toxicol. Sci.*, **77**, 126.
3. Zhang, B.T., Zheng, X., Li, H.F., and Lin, J.M. (2013) *Anal. Chim. Acta*, **784**, 1.
4. Lin, T., Bajpai, V., Ji, T., and Dai, L. (2003) *Aust. J. Chem.*, **56**, 635.
5. Maynard, A.D., Baron, P.A., Foley, M., Shvedova, A.A., Kisin, E.R., and Castranova, V. (2004) *J. Toxicol. Environ. Health A*, **67**, 87.
6. Johnson, D.R., Methner, M.M., Kennedy, A.J., and Steevens, J.A. (2010) *Environ. Health Perspect.*, **118**, 49.
7. Han, J.H., Lee, E.J., Lee, J.H., So, K.P., Lee, Y.H., Bae, G.N., Lee, S.B., Ji, J.H., Cho, M.H., and Yu, I.J. (2008) *Inhalation Toxicol.*, **20**, 741.
8. Methner, M.M. (2008) *J. Occup. Environ. Hyg.*, **5**, D63.
9. Maynard, A. and Kuempel, E.D. (2005) *J. Nanopart. Res.*, **7**, 587.
10. McClellan, R.O. (2000) in *Particle-Lung Interactions*, 1st edn (eds P. Gehr and J. Heyder), Marcel Dekker.
11. Castranova, V. (2011) *J. Occup. Environ. Med./Am. Coll. Occup. Environ. Med.*, **53**, S14.
12. Kumar, V., Kumari, A., Guleria, P., and Yadav, S.K. (2012) *Rev. Environ. Contam. Toxicol.*, **215**, 39.
13. Donaldson, K., Aitken, R., Tran, L., Stone, V., Duffin, R., Forrest, G., and Alexander, A. (2006) *Toxicol. Sci.*, **92**, 5.
14. Xu, J., Alexander, D.B., Futakuchi, M., Numano, T., Fukamachi, K., Suzui, M., Omori, T., Kanno, J., Hirose, A., and Tsuda, H. (2014) *Cancer Sci.*, **105**, 763.
15. Morimoto, Y., Horie, M., Kobayashi, N., Shinohara, N., and Shimada, M. (2013) *Acc. Chem. Res.*, **46**, 770.
16. Pacurari, M., Castranova, V., and Vallyathan, V. (2010) *J. Toxicol. Environ. Health A*, **73**, 378.
17. Rodriguez, N.M., Chambers, A., and Baker, R.T.K. (1995) *Langmuir*, **11**, 3862.
18. Hamilton, R.F. Jr., Wu, Z., Mitra, S., Shaw, P.K., and Holian, A. (2013) *Part. Fibre Toxicol.*, **10**, 57.
19. Donaldson, K. and Tran, C.L. (2002) *Inhalation Toxicol.*, **14**, 5.
20. Tran, C.L., Buchanan, D., Cullen, R.T., Searl, A., Jones, A.D., and Donaldson, K. (2000) *Inhal. Toxicol.*, **12**, 1113.
21. Duffin, R., Tran, C.L., Clouter, A., Brown, D.M., Macnee, W., Stone, V., and Donaldson, K. (2002) *Ann. Occup. Hyg.*, **46**, 242.
22. Poulsen, S.S., Saber, A.T., Williams, A., Andersen, O., Kobler, C., Atluri, R., Pozzebon, M.E., Mucelli, S.P., Simion, M., Rickerby, D., Mortensen, A., Jackson, P., Kyjovska, Z.O., Molhave, K., Jacobsen, N.R., Jensen, K.A., Yauk, C.L., Wallin, H., Halappanavar, S., and Vogel, U. (2015) *Toxicol. Appl. Pharmacol.*, **284**, 16.
23. Mercer, R.R., Scabilloni, J., Wang, L., Kisin, E., Murray, A.R., Schwegler-Berry, D., Shvedova, A.A., and Castranova, V. (2008) *Am. J. Physiol. Lung Cell. Mol. Physiol.*, **294**, L87.
24. Shvedova, A.A., Kisin, E., Murray, A.R., Johnson, V.J., Gorelik, O., Arepalli, S., Hubbs, A.F., Mercer, R.R., Keohavong, P., Sussman, N., Jin, J., Yin, J., Stone, S., Chen, B.T., Deye, G., Maynard, A., Castranova, V., Baron, P.A., and Kagan, V.E. (2008) *Am. J. Physiol. Lung Cell. Mol. Physiol.*, **295**, L552.
25. Shvedova, A.A., Kisin, E.R., Mercer, R., Murray, A.R., Johnson, V.J., Potapovich, A.I., Tyurina, Y.Y., Gorelik, O., Arepalli, S., Schwegler-Berry, D., Hubbs, A.F., Antonini, J., Evans, D.E., Ku, B.K., Ramsey, D., Maynard, A., Kagan, V.E., Castranova, V., and Baron, P. (2005) *Am. J. Physiol. Lung Cell. Mol. Physiol.*, **289**, L698.
26. Shvedova A.A., Sager T., Murray A.R., Kisin E., Porter D.W., Leonard S.S., Schwegler Berry D., Robinson V.A., Castranova V. (2007) Critical issues in the evaluation of possible effects resulting from airborne nanoparticles. Nanotoxicology: Characterization, Dosing and Health Effects. *Monteiro-Riviere*

10.1002/9783527692866.ch6, Downloaded from https://onlinelibrary.wiley.com/doi/10.1002/9783527692866.ch6 by NASA Shared Services Center (NSSC), Wiley Online Library on [19/05/2023]. See the Terms and Conditions (https://onlinelibrary.wiley.com/terms-and-conditions) on Wiley Online Library for rules of use; OA articles are governed by the applicable Creative Commons License

NA, Tran CL, eds., New York: Informa Healthcare:225–236.
27. Ellinger-Ziegelbauer, H. and Pauluhn, J. (2009) *Toxicology*, **266**, 16.
28. Kreyling, W.G., Semmler-Behnke, M., Seitz, J., Scymczak, W., Wenk, A., Mayer, P., Takenaka, S., and Oberdorster, G. (2009) *Inhalation Toxicol.*, **21** (Suppl. 1), 55.
29. Aijaz, S., Balda, M.S., and Matter, K. (2006) *Int. Rev. Cytol.*, **248**, 261.
30. Maier, M., Hannebauer, B., Holldorff, H., and Albers, P. (2006) *J. Occup. Environ. Med./Am. Coll. Occup. Environ. Med.*, **48**, 1314.
31. Porter, D.W., Sriram, K., Wolfarth, M.G., Jefferson, A., Schwegler-Berry, D., Andrew, M., and Castranova, V. (2008) *Nanotoxicology*, **2**, 144.
32. Wang, L., Mercer, R.R., Rojanasakul, Y., Qiu, A., Lu, Y., Scabilloni, J.F., Wu, N., and Castranova, V. (2010) *J. Toxicol. Environ. Health A*, **73**, 410.
33. Mercer, R.R., Scabilloni, J.F., Hubbs, A.F., Battelli, L.A., McKinney, W., Friend, S., Wolfarth, M.G., Andrew, M., Castranova, V., and Porter, D.W. (2013) *Part. Fibre Toxicol.*, **10**, 33.
34. Mercer, R.R., Scabilloni, J.F., Hubbs, A.F., Wang, L., Battelli, L.A., McKinney, W., Castranova, V., and Porter, D.W. (2013) *Part. Fibre Toxicol.*, **10**, 38.
35. Castranova, V., Porter, D., and Mercer, R. (2015) in *Nanoparticles in the Lung: Environmental Exposure and Drug Delivery* (eds A. Tsuda and P. Gehr), CRC Press.
36. Poland, C.A., Duffin, R., Kinloch, I., Maynard, A., Wallace, W.A., Seaton, A., Stone, V., Brown, S., Macnee, W., and Donaldson, K. (2008) *Nat. Nanotechnol.*, **3**, 423.
37. van Berlo, D., Wilhelmi, V., Boots, A.W., Hullmann, M., Kuhlbusch, T.A., Bast, A., Schins, R.P., and Albrecht, C. (2014) *Arch. Toxicol.*, **88** (9): 1725–37.
38. Manke, A., Luanpitpong, S., Dong, C., Wang, L., He, X., Battelli, L., Derk, R., Stueckle, T.A., Porter, D.W., Sager, T., Gou, H., Dinu, C.Z., Wu, N., Mercer, R.R., and Rojanasakul, Y. (2014) *Int. J. Mol. Sci.*, **15**, 7444.
39. Shvedova, A.A., Yanamala, N., Kisin, E.R., Tkach, A.V., Murray, A.R., Hubbs, A., Chirila, M.M., Keohavong, P., Sycheva, L.P., Kagan, V.E., and Castranova, V. (2014) *Am. J. Physiol. Lung Cell. Mol. Physiol.*, **306**, L170.
40. Taylor, A.J., McClure, C.D., Shipkowski, K.A., Thompson, E.A., Hussain, S., Garantziotis, S., Parsons, G.N., and Bonner, J.C. (2014) *PLoS One*, **9**, e106870.
41. Kotchey, G.P., Zhao, Y., Kagan, V.E., and Star, A. (2013) *Adv. Drug Deliv. Rev.*, **65** (15): 1921–32.
42. Zhao, Y., Allen, B.L., and Star, A. (2011) *J. Phys. Chem. A*, **115**, 9536.
43. Li, R., Wang, X., Ji, Z., Sun, B., Zhang, H., Chang, C.H., Lin, S., Meng, H., Liao, Y.P., Wang, M., Li, Z., Hwang, A.A., Song, T.B., Xu, R., Yang, Y., Zink, J.I., Nel, A.E., and Xia, T. (2013) *ACS Nano*, **7**, 2352.
44. Sager, T.M., Wolfarth, M.W., Andrew, M., Hubbs, A., Friend, S., Chen, T.H., Porter, D.W., Wu, N., Yang, F., Hamilton, R.F., and Holian, A. (2014) *Nanotoxicology*, **8**, 317.
45. Oberdorster, G., Oberdorster, E., and Oberdorster, J. (2005) *Environ. Health Perspect.*, **113**, 823.
46. Takenaka, S., Karg, E., Kreyling, W.G., Lentner, B., Moller, W., Behnke-Semmler, M., Jennen, L., Walch, A., Michalke, B., Schramel, P., Heyder, J., and Schulz, H. (2006) *Inhalation Toxicol.*, **18**, 733.
47. Mercer, R.R., Hubbs, A.F., Scabilloni, J.F., Wang, L., Battelli, L.A., Schwegler-Berry, D., Castranova, V., and Porter, D.W. (2010) *Part. Fibre Toxicol.*, **7**, 28.
48. Mercer, R.R., Hubbs, A.F., Scabilloni, J.F., Wang, L., Battelli, L.A., Friend, S., Castranova, V., and Porter, D.W. (2011) *Part. Fibre Toxicol.*, **8**, 21.
49. Li, J.G., Li, W.X., Xu, J.Y., Cai, X.Q., Liu, R.L., Li, Y.J., Zhao, Q.F., and Li, Q.N. (2007) *Environ. Toxicol.*, **22**(4), 415–21.
50. Semmler-Behnke, M., Takenaka, S., Fertsch, S., Wenk, A., Seitz, J., Mayer, P., Oberdorster, G., and Kreyling, W.G. (2007) *Environ. Health Perspect.*, **115**, 728.
51. Ryman-Rasmussen, J.P., Cesta, M.F., Brody, A.R., Shipley-Phillips, J.K.,

10.1002/9783527692866.ch6, Downloaded from https://onlinelibrary.wiley.com/doi/10.1002/9783527692866.ch6 by NASA Shared Services Center (NSSC), Wiley Online Library on [19/05/2023]. See the Terms and Conditions (https://onlinelibrary.wiley.com/terms-and-conditions) on Wiley Online Library for rules of use; OA articles are governed by the applicable Creative Commons License

Everitt, J.I., Tewksbury, E.W., Moss, O.R., Wong, B.A., Dodd, D.E., Andersen, M.E., and Bonner, J.C. (2009) *Nat. Nanotechnol.*, **4**, 747.

52. Porter, D.W., Hubbs, A.F., Mercer, R.R., Wu, N., Wolfarth, M.G., Sriram, K., Leonard, S., Battelli, L., Schwegler-Berry, D., Friend, S., Andrew, M., Chen, B.T., Tsuruoka, S., Endo, M., and Castranova, V. (2010) *Toxicology*, **269**, 136.
53. Xu, J., Futakuchi, M., Shimizu, H., Alexander, D.B., Yanagihara, K., Fukamachi, K., Suzui, M., Kanno, J., Hirose, A., Ogata, A., Sakamoto, Y., Nakae, D., Omori, T., and Tsuda, H. (2012) *Cancer Sci.*, **103**, 2045.
54. Andujar, P., Lanone, S., Brochard, P., and Boczkowski, J. (2011) *Rev. Mal. Respir.*, **28**, e66.
55. Oberdorster, G. (2004) First International Symposium on Occupational Health Implications of Nanomaterials, Buxton, Derbyshire, UK, http://www.hsl.gov.uk/media/394200/nanosymrep_final.pdf
56. Moller, W., Felten, K., Sommerer, K., Scheuch, G., Meyer, G., Meyer, P., Haussinger, K., and Kreyling, W.G. (2008) *Am. J. Respir. Crit. Care Med.*, **177**, 426.
57. Oberdorster, G., Sharp, Z., Atudorei, V., Elder, A., Gelein, R., Lunts, A., Kreyling, W., and Cox, C. (2002) *J. Toxicol. Environ. Health A*, **65**, 1531.
58. Nemmar, A., Vanbilloen, H., Hoylaerts, M.F., Hoet, P.H., Verbruggen, A., and Nemery, B. (2001) *Am. J. Respir. Crit. Care Med.*, **164**, 1665.
59. Aiso, S., Kubota, H., Umeda, Y., Kasai, T., Takaya, M., Yamazaki, K., Nagano, K., Sakai, T., Koda, S., and Fukushima, S. (2011) *Ind. Health*, **49**, 215.
60. Czarny, B., Georgin, D., Berthon, F., Plastow, G., Pinault, M., Patriarche, G., Thuleau, A., L'Hermite, M.M., Taran, F., and Dive, V. (2014) *ACS Nano*, **8**, 5715.
61. Reddy, A.R., Krishna, D.R., Reddy, Y.N., and Himabindu, V. (2010) *Toxicol. Mech. Methods*, **20**, 267.
62. Porter, D.W., Hubbs, A.F., Chen, B.T., McKinney, W., Mercer, R.R., Wolfarth, M.G., Battelli, L., Wu, N., Sriram, K., Leonard, S., Andrew, M., Willard, P., Tsuruoka, S., Endo, M., Tsukada, T., Munekane, F., Frazer, D.G., and Castranova, V. (2013) *Nanotoxicology*, **7**, 1179.
63. Stapleton, P.A., Minarchick, V.C., Cumpston, A.M., McKinney, W., Chen, B.T., Sager, T.M., Frazer, D.G., Mercer, R.R., Scabilloni, J., Andrew, M.E., Castranova, V., and Nurkiewicz, T.R. (2012) *Int. J. Mol. Sci.*, **13**, 13781.
64. Ishimatsu, S., Hori, H., Kasai, T., Ogami, A., Morimoto, Y., Oyabu, T., and Tanaka, I. (2009) *Inhalation Toxicol.*, **21**, 668.
65. Oyabu, T., Myojo, T., Morimoto, Y., Ogami, A., Hirohashi, M., Yamamoto, M., Todoroki, M., Mizuguchi, Y., Hashiba, M., Lee, B.W., Shimada, M., Wang, W.N., Uchida, K., Endoh, S., Kobayashi, N., Yamamoto, K., Fujita, K., Mizuno, K., Inada, M., Nakazato, T., Nakanishi, J., and Tanaka, I. (2011) *Inhalation Toxicol.*, **23**, 784.
66. Kagan, V.E., Kapralov, A.A., Croix, C.M.S., Watkins, S.C., Kisin, E.R., Kotchey, G.P., Balasubramanian, K., Vlasova, I.I., Yu, J., Kim, K., Seo, W., Mallampalli, R.K., Star, A., and Shvedova, A.A. (2014) *ACS Nano*, **8**, 5610.
67. Erdely, A., Hulderman, T., Salmen, R., Liston, A., Zeidler-Erdely, P.C., Schwegler-Berry, D., Castranova, V., Koyama, S., Kim, Y.A., Endo, M., and Simeonova, P.P. (2009) *Nano Lett.*, **9**, 36.
68. Sargent, L.M., Porter, D.W., Staska, L.M., Hubbs, A.F., Lowry, D.T., Battelli, L., Siegrist, K.J., Kashon, M.L., Mercer, R.R., Bauer, A.K., Chen, B.T., Salisbury, J.L., Frazer, D., McKinney, W., Andrew, M., Tsuruoka, S., Endo, M., Fluharty, K.L., Castranova, V., and Reynolds, S.H. (2014) *Part. Fibre Toxicol.*, **11**, 3.
69. Kobler, C., Poulsen, S.S., Saber, A.T., Jacobsen, N.R., Wallin, H., Yauk, C.L., Halappanavar, S., Vogel, U., Qvortrup, K., and Molhave, K. (2015) *PLoS One*, **10**, e0116481.
70. Schreiber, N., Strobele, M., Kopf, J., Hochscheid, R., Kotte, E., Weber, P., Hansen, T., Bockhorn, H., and Muller, B. (2013) *J. Toxicol. Environ. Health A*, **76**, 1317.

10.1002/9783527692866.ch6, Downloaded from https://onlinelibrary.wiley.com/doi/10.1002/9783527692866.ch6 by NASA Shared Services Center (NSSC), Wiley Online Library on [19/05/2023]. See the Terms and Conditions (https://onlinelibrary.wiley.com/terms-and-conditions) on Wiley Online Library for rules of use; OA articles are governed by the applicable Creative Commons License

71. Zhang, R., Dai, Y., Zhang, X., Niu, Y., Meng, T., Li, Y., Duan, H., Bin, P., Ye, M., Jia, X., Shen, M., Yu, S., Yang, X., Gao, W., and Zheng, Y. (2014) *Part. Fibre Toxicol.*, **11**, 73.
72. Lee, J.S., Choi, Y.C., Shin, J.H., Lee, J.H., Lee, Y., Park, S.Y., Baek, J.E., Park, J.D., Ahn, K., and Yu, I.J. (2014) *Nanotoxicology*, 1.
73. Mangum, J.B., Turpin, E.A., Antao-Menezes, A., Cesta, M.F., Bermudez, E., and Bonner, J.C. (2006) *Part. Fibre Toxicol.*, **3**, 15.
74. Kasai, T., Umeda, Y., Ohnishi, M., Kondo, H., Takeuchi, T., Aiso, S., Nishizawa, T., Matsumoto, M., and Fukushima, S. (2014) *Nanotoxicology*, 1.
75. Muller, J., Huaux, F., Moreau, N., Misson, P., Heilier, J.F., Delos, M., Arras, M., Fonseca, A., Nagy, J.B., and Lison, D. (2005) *Toxicol. Appl. Pharmacol.*, **207**, 221.
76. Warheit, D.B., Laurence, B.R., Reed, K.L., Roach, D.H., Reynolds, G.A., and Webb, T.R. (2004) *Toxicol. Sci.*, **77**, 117.
77. Huizar, I., Malur, A., Midgette, Y.A., Kukoly, C., Chen, P., Ke, P.C., Podila, R., Rao, A.M., Wingard, C.J., Dobbs, L., Barna, B.P., Kavuru, M.S., and Thomassen, M.J. (2011) *Am. J. Respir. Cell Mol. Biol.*, **45**, 858.
78. Inoue, K., Koike, E., Yanagisawa, R., Hirano, S., Nishikawa, M., and Takano, H. (2009) *Toxicol. Appl. Pharmacol.*, **237**, 306.
79. Park, E.J., Cho, W.S., Jeong, J., Yi, J., Choi, K., and Park, K. (2009) *Toxicology*, **259**, 113.
80. Ryman-Rasmussen, J.P., Tewksbury, E.W., Moss, O.R., Cesta, M.F., Wong, B.A., and Bonner, J.C. (2009) *Am. J. Respir. Cell Mol. Biol.*, **40**, 349.
81. Ronzani C., Casset A., Pons F. (2014) *Arch Toxicol.*, **88**(2):489–99.
82. Todd, N.W., Luzina, I.G., and Atamas, S.P. (2012) *Fibrogenesis Tissue Repair*, **5**, 11.
83. Sager, T.M., Wolfarth, M.W., Battelli, L.A., Leonard, S.S., Andrew, M., Steinbach, T., Endo, M., Tsuruoka, S., Porter, D.W., and Castranova, V. (2013) *J. Toxicol. Environ. Health A*, **76**, 922.
84. Li, Z., Hulderman, T., Salmen, R., Chapman, R., Leonard, S.S., Young, S.H., Shvedova, A., Luster, M.I., and Simeonova, P.P. (2007) *Environ. Health Perspect.*, **115**, 377.
85. Shvedova, A.A., Kisin, E.R., Murray, A.R., Gorelik, O., Arepalli, S., Castranova, V., Young, S.H., Gao, F., Tyurina, Y.Y., Oury, T.D., and Kagan, V.E. (2007) *Toxicol. Appl. Pharmacol.*, **221**, 339.
86. Shvedova, A.A., Kisin, E.R., Murray, A.R., Mouithys-Mickalad, A., Stadler, K., Mason, R.P., and Kadiiska, M. (2014) *Free Radic. Biol. Med.*, **73**, 154.
87. Kyjovska, Z.O., Jacobsen, N.R., Saber, A.T., Bengtson, S., Jackson, P., Wallin, H., and Vogel, U. (2015) *Environ. Mol. Mutagen.*, **56**, 41.
88. Bourdon, J.A., Saber, A.T., Jacobsen, N.R., Jensen, K.A., Madsen, A.M., Lamson, J.S., Wallin, H., Moller, P., Loft, S., Yauk, C.L., and Vogel, U.B. (2012) *Part. Fibre Toxicol.*, **9**, 5.
89. Bourdon, J.A., Saber, A.T., Jacobsen, N.R., Williams, A., Vogel, U., Wallin, H., Halappanavar, S., and Yauk, C.L. (2013) *Cardiovasc. Toxicol.*, **13**, 406.
90. Wang, L., Luanpitpong, S., Castranova, V., Tse, W., Lu, Y., Pongrakhananon, V., and Rojanasakul, Y. (2011) *Nano Lett.*, **11**, 2796.
91. Takagi, A., Hirose, A., Nishimura, T., Fukumori, N., Ogata, A., Ohashi, N., Kitajima, S., and Kanno, J. (2008) *J. Toxicol. Sci.*, **33**, 105.
92. Shvedova, A.A., Kisin, E.R., Yanamala, N., Tkach, A.V., Gutkin, D.W., Star, A., Shurin, G.V., Kagan, V.E., and Shurin, M.R. (2015) *Cancer Res.*, 15;**75**(8):1615–23.
93. Donaldson, K., Murphy, F.A., Duffin, R., and Poland, C.A. (2010) *Part. Fibre Toxicol.*, **7**, 5.
94. Murphy, F.A., Poland, C.A., Duffin, R., Al-Jamal, K.T., Ali-Boucetta, H., Nunes, A., Byrne, F., Prina-Mello, A., Volkov, Y., Li, S., Mather, S.J., Bianco, A., Prato, M., Macnee, W., Wallace, W.A., Kostarelos, K., and Donaldson, K. (2011) *Am. J. Pathol.*, **178**, 2587.
95. Poland, C.A., Byrne, F., Cho, W.S., Prina-Mello, A., Murphy, F.A., Davies, G.L., Coey, J.M., Gounko, Y., Duffin, R.,

10.1002/9783527692866.ch6, Downloaded from https://onlinelibrary.wiley.com/doi/10.1002/9783527692866.ch6 by NASA Shared Services Center (NSSC), Wiley Online Library on [19/05/2023]. See the Terms and Conditions (https://onlinelibrary.wiley.com/terms-and-conditions) on Wiley Online Library for rules of use; OA articles are governed by the applicable Creative Commons License

Volkov, Y., and Donaldson, K. (2011) *Nanotoxicology*, **6**, 899.

96. Grosse, Y., Loomis, D., Guyton, K.Z., Lauby-Secretan, B., Ghissassi, E., Bouvard, V., Benbrahim-Tallaa, L., Guha, N., Scoccianti, C., Mattock, H., Straif, K., International Agency for Research on Cancer Monograph Working Group, and International Agency for Reseach on Cancer (2014) *Lancet Oncol.*, **15**(13):1427–8.
97. Baan, R., Straif, K., Grosse, Y., Secretan, B., El Ghissassi, F., Cogliano, V., and WHO International Agency for Research on Cancer Monograph Working Group (2006) *Lancet Oncol.*, **7**, 295.
98. Roller, M. (2009) *Inhal. Toxicol.*, **21** (Suppl. 1), 144.
99. Baan, R.A. (2007) *Inhal. Toxicol.*, **19** (Suppl. 1), 213.
100. Kuempel, E.D., Tran, C.L., Castranova, V., and Bailer, A.J. (2006) *Inhal. Toxicol.*, **18**, 717.
101. Donaldson, K., Duffin, R., Langrish, J.P., Miller, M.R., Mills, N.L., Poland, C.A., Raftis, J., Shah, A., Shaw, C.A., and Newby, D.E. (2013) *Nanomedicine (Lond.)*, **8**, 403.
102. Saber, A.T., Jacobsen, N.R., Jackson, P., Poulsen, S.S., Kyjovska, Z.O., Halappanavar, S., Yauk, C.L., Wallin, H., and Vogel, U. (2014) *Wiley Interdiscip. Rev. Nanomed. Nanobiotechnol.*, **6**, 517.
103. Saber, A.T., Lamson, J.S., Jacobsen, N.R., Ravn-Haren, G., Hougaard, K.S., Nyendi, A.N., Wahlberg, P., Madsen, A.M., Jackson, P., Wallin, H., and Vogel, U. (2013) *PLoS One*, **8**, e69020.
104. Husain, M., Saber, A.T., Guo, C., Jacobsen, N.R., Jensen, K.A., Yauk, C.L., Williams, A., Vogel, U., Wallin, H., and Halappanavar, S. (2013) *Toxicol. Appl. Pharmacol.*, **269**, 250.
105. Saber, A.T., Halappanavar, S., Folkmann, J.K., Bornholdt, J., Boisen, A.M., Moller, P., Williams, A., Yauk, C., Vogel, U., Loft, S., and Wallin, H. (2009) *Part. Fibre Toxicol.*, **6**, 12.
106. Jackson, P., Halappanavar, S., Hougaard, K.S., Williams, A., Madsen, A.M., Lamson, J.S., Andersen, O., Yauk, C., Wallin, H., and Vogel, U. (2013) *Nanotoxicology*, **7**, 85.
107. Jackson, P., Hougaard, K.S., Vogel, U., Wu, D., Casavant, L., Williams, A., Wade, M., Yauk, C.L., Wallin, H., and Halappanavar, S. (2012) *Mutat. Res.*, **745**, 73.
108. Sos Poulsen, S., Jacobsen, N.R., Labib, S., Wu, D., Husain, M., Williams, A., Bogelund, J.P., Andersen, O., Kobler, C., Molhave, K., Kyjovska, Z.O., Saber, A.T., Wallin, H., Yauk, C.L., Vogel, U., and Halappanavar, S. (2013) *PLoS One*, **8**, e80452.
109. Halappanavar, S., Jackson, P., Williams, A., Jensen, K.A., Hougaard, K.S., Vogel, U., Yauk, C.L., and Wallin, H. (2011) *Environ. Mol. Mutagen.*, **52**, 425.
110. Lam, C.W., James, J.T., McCluskey, R., Arepalli, S., and Hunter, R.L. (2006) *Crit. Rev. Toxicol.*, **36**, 189.
111. Xu, J.-Y., Li, Q.-N., Li, J.-G., Ran, T.-C., Wu, S.-W., Song, W.-M., Chen, S.-L., and Li, W.-X. (2007) *Carbon*, **45**, 1865.
112. Roberts, J.R., Kenyon, A., Leonard, S.S., Fix, N.R., Porter, D.W., Sager, T., Wolfarth, M.G., Yingling, B.M., Chaudhuri, I.S., Kyrlidis, A., Bilgesu, S.A., Mercer, R.R., Schwegler-Berry, D., Castranova, V., and Erdely, A. (2013) Toxicologist., **132** (1): 98.

10.1002/9783527692866.ch6, Downloaded from https://onlinelibrary.wiley.com/doi/10.1002/9783527692866.ch6 by NASA Shared Services Center (NSSC), Wiley Online Library on [19/05/2023]. See the Terms and Conditions (https://onlinelibrary.wiley.com/terms-and-conditions) on Wiley Online Library for rules of use; OA articles are governed by the applicable Creative Commons License